NATIONAL ADVISORY COMMITTEE FOR AERONAUTICS

REPORT 938

SUMMARY OF SECTION DATA ON TRAILING-EDGE HIGH-LIFT DEVICES

By JONES F. CAHILL

1949

For sale by the Superintendent of Documents, U. S. Government Printing Office, Washington 25, D. C. Yearly subscription, $3; foreign, $4.50; single copy price varies according to size - - - - - - - - - - Price 25 cents

AERONAUTIC SYMBOLS

1. FUNDAMENTAL AND DERIVED UNITS

	Symbol	Metric		English	
		Unit	Abbreviation	Unit	Abbreviation
Length	l	meter	m	foot (or mile)	ft (or mi)
Time	t	second	s	second (or hour)	sec (or hr)
Force	F	weight of 1 kilogram	kg	weight of 1 pound	lb
Power	P	horsepower (metric)		horsepower	hp
Speed	V	kilometers per hour	kph	miles per hour	mph
		meters per second	mps	feet per second	fps

2. GENERAL SYMBOLS

W Weight$=mg$

g Standard acceleration of gravity$=9.80665$ m/s^2 or 32.1740 ft/sec^2

m Mass$=\frac{W}{g}$

I Moment of inertia$=mk^2$. (Indicate axis of radius of gyration k by proper subscript.)

μ Coefficient of viscosity

ν Kinematic viscosity

ρ Density (mass per unit volume)

Standard density of dry air, 0.12497 kg-m^{-4}-s^2 at 15° C and 760 mm; or 0.002378 lb-ft^{-4} sec^2

Specific weight of "standard" air, 1.2255 kg/m^3 or 0.07651 lb/cu ft

3. AERODYNAMIC SYMBOLS

S Area

S_w Area of wing

G Gap

b Span

c Chord

A Aspect ratio, $\frac{b^2}{S}$

V True air speed

q Dynamic pressure, $\frac{1}{2}\rho V^2$

L Lift, absolute coefficient $C_L=\frac{L}{qS}$

D Drag, absolute coefficient $C_D=\frac{D}{qS}$

D_0 Profile drag, absolute coefficient $C_{D_0}=\frac{D_0}{qS}$

D_i Induced drag, absolute coefficient $C_{D_i}=\frac{D_i}{qS}$

D_p Parasite drag, absolute coefficient $C_{D_p}=\frac{D_p}{qS}$

C Cross-wind force, absolute coefficient $C_C=\frac{C}{qS}$

i_w Angle of setting of wings (relative to thrust line)

i_t Angle of stabilizer setting (relative to thrust line)

Q Resultant moment

Ω Resultant angular velocity

R Reynolds number, $\rho\frac{Vl}{\mu}$ where l is a linear dimension (e.g., for an airfoil of 1.0 ft chord, 100 mph, standard pressure at 15° C, the corresponding Reynolds number is 935,400; or for an airfoil of 1.0 m chord, 100 mps, the corresponding Reynolds number is 6,865,000)

α Angle of attack

ϵ Angle of downwash

α_0 Angle of attack, infinite aspect ratio

α_i Angle of attack, induced

α_a Angle of attack, absolute (measured from zero-lift position)

γ Flight-path angle

REPORT 938

SUMMARY OF SECTION DATA ON TRAILING-EDGE HIGH-LIFT DEVICES

By JONES F. CAHILL

Langley Aeronautical Laboratory
Langley Air Force Base, Va.

National Advisory Committee for Aeronautics

Headquarters, 1724 F Street NW., Washington 25, D. C.

Created by act of Congress approved March 3, 1915, for the supervision and direction of the scientific study of the problems of flight (U. S. Code, title 50, sec. 151). Its membership was increased from 12 to 15 by act approved March 2, 1929, and to 17 by act approved May 25, 1948. The members are appointed by the President, and serve as such without compensation.

REPORT 938

SUMMARY OF SECTION DATA ON TRAILING-EDGE HIGH-LIFT DEVICES

By JONES F. CAHILL

SUMMARY

A summary has been made of available data on the characteristics of airfoil sections with trailing-edge high-lift devices. Data for plain, split, and slotted flaps are collected and analyzed. The effects of each of the variables involved in the design of the various types of flap are examined and, in cases where sufficient data are given, optimum configurations are deduced. Wherever possible, the effects of airfoil section, Reynolds number, and leading-edge roughness are shown. For single and double slotted flaps, where a large amount of unrelated data are available, maximum lift coefficients of many configurations are presented in tables.

INTRODUCTION

A rather large amount of data on the section aerodynamic characteristics of trailing-edge flaps has been obtained during the course of the last several years. Some of the data has been obtained as a part of a general program on the investigation of these characteristics; but a large amount, particularly that obtained during the war, has of necessity been directed toward the development of high-lift devices for specific airplanes and, as a result, is generally unrelated to the over-all program. This report is prepared with a view of collecting and correlating, insofar as possible, the data that are available for the purpose of providing a guide for the selection of the type or size of high-lift device for specific applications and for showing, if possible, means for predicting the characteristics of configurations which have not been specifically tested.

In some few cases, the only data available to show the effects of fundamental flap design parameters were obtained on rectangular wings of constant section and of aspect ratio 6. In all other cases, only section data have been included in this report, both in an attempt to keep the size of the report below a reasonable limit and because of the fact that the application of the section data to finite span wings can be considered a separate problem. For this reason, no data are shown on the effects of flap tips, on cut-outs, on fuselage interference, or on slipstream effects. No detailed analyses have been made on the effects of the flap characteristics on the performance of airplanes.

Although the requirements of good high-lift devices are fairly well known, a short summary of the more important characteristics is presented herein. The increase in maximum lift coefficient is the primary function of flaps; and, generally, the effects of flaps on other characteristics must be considered as secondary results of this increase in maximum lift.

Flaps and other high-lift devices were first put into use for landing airplanes in small airfields with nearby obstructions without penalizing high-speed performance. The recent use of higher and higher wing loadings has made the need for these devices even more acute and has presented the necessity for using high-lift devices during take-off as well as landing. For take-off, a high maximum lift is desirable but must be accompanied by low drags. For landing, the highest maximum lift possible is desirable for decreasing the landing speed, and some additional drag is useful for steepening the glide path for landings over high obstructions. Recent flight tests (reference 1), however, have shown that the pilot's judgment is seriously impaired if the rate of descent during landing is greater than about 25 feet per second. Too high a drag coefficient therefore cannot be tolerated.

In addition to these fundamental requirements, the flap should be such that in its retracted position it adds as little as possible to the drag of the wing. High pitching-moment coefficients are undesirable both because of the structural requirements of the wing and because of the fact that the down load on the tail required to trim out the pitching moment detracts from the lift of the wing. Low aerodynamic loads on the flaps are desirable both from strength considerations and operating requirements. Both the pitching moments and the flap loads are a direct result, however, of the same phenomena that produce the lift, and very little can be done to reduce either of these for a given type of flap.

SYMBOLS

c	airfoil chord
x	distance along airfoil chord
c_a	slot-lip extension, distance along chord line from leading edge to end of slot lip, fraction of airfoil chord
c_f/c	flap-chord ratio
c_v/c	vane-chord ratio
t/c	airfoil thickness ratio
C_L	lift coefficient
$C_{L_{max}}$	maximum lift coefficient
c_l	section lift coefficient
c_{l_i}	design section lift coefficient
$c_{l_{max}}$	maximum section lift coefficient
$\Delta c_{l_{max}}$	increment of maximum section lift coefficient
$\Delta c_{l_{max_{opt}}}$	optimum increment of maximum section lift coefficient, highest maximum lift coefficient measured for a given airfoil-flap combination
q	stream dynamic pressure

P coefficient of pressure difference across airfoil ($S_U - S_L$, where S_U and S_L are surface pressure coefficients on the upper and lower surfaces of the airfoil at a given point along the chord)

b variation of hinge-moment coefficient with flap deflection $\left(\frac{1}{2}\frac{dc_h}{d\delta}\right)$

b_1/a_1 variation of hinge-moment coefficient with lift coefficient (dc_h/dc_l)

η variation of flap normal-force coefficient with flap deflection ($dc_n/d\delta$)

η_0 variation of flap normal-force coefficient with lift coefficient (dc_n/dc_l)

C_D drag coefficient

c_d section drag coefficient

c_m section pitching-moment coefficient

c_{m_f} flap section moment coefficient

c_{h_f} flap section hinge-moment coefficient

c_{c_f} flap section chord-force coefficient

c_{n_f} flap section normal-force coefficient

Δc_{n_f} increment of flap section normal-force coefficient

δ_f flap deflection

δ_v vane deflection

c_{m_v} vane section moment coefficient

c_{c_v} vane section chord-force coefficient

c_{n_v} vane section normal-force coefficient

x_f, y_f horizontal and vertical positions of flap leading edge (figs. 24 and 40)

x_v, y_v horizontal and vertical positions of vane leading edge (fig. 40)

$\frac{\Delta c_m}{\Delta c_l}$ ratio of incremental pitching-moment coefficient to incremental section lift coefficient caused by flap deflection

R Reynolds number

A aspect ratio

α_0 section angle of attack

FLAP THEORY

The basic theoretical treatment of the effects of flaps on the characteristics of airfoils was made by Glauert (references 2 and 3) by an extension of the thin-airfoil theory. This analysis led to expressions by which the lift, pitching moment, and flap hinge moments can be calculated. This thin-airfoil theory gives the value of the pressure difference at any point x along the chord for the airfoil with flap deflected in terms of the stream dynamic pressure q as:

$$P=\frac{4(1+\cos\theta)}{\sin\theta}\left(\alpha+\frac{\pi-\theta_0}{\pi}\delta\right)+\sum_{n=1}^{\infty}\frac{8\delta\sin n\theta_0\sin n\theta}{n\pi}$$

and for the flap neutral case:

$$P_1=\frac{4(1+\cos\theta)}{\sin\theta}\alpha$$

The incremental load distribution caused by flap deflection is then

$$P_\delta=\left[\frac{4(1+\cos\theta)(\pi-\theta_0)}{\pi\sin\theta}+\sum_{n=1}^{\infty}\frac{8\sin n\theta_0\sin n\theta}{n\pi}\right]\delta$$

where

$\theta=\cos^{-1}\left(1-\frac{2x}{c}\right)$

α angle of attack measured to undeflected part of chord line

x distance along chord from leading edge

θ_0 value of θ at flap hinge

$\cos\theta_0=-(1-2E)$

$\sin\theta_0=2\sqrt{E(1-E)}$

E ratio of flap chord to total airfoil chord (c_f/c)

δ flap deflection

Definitions of the parameters α, δ, and E are shown in figure 1. This incremental load distribution may now be considered as the sum of two components, an incremental additional distribution and an incremental basic distribution; thus,

$$P_{a_\delta}=\frac{4(\pi-\theta_0)(1+\cos\theta)}{\pi\sin\theta}\delta$$

and

$$P_{b_\delta}=\left(\sum_{n=1}^{\infty}\frac{8\sin n\theta_0\sin n\theta}{n\pi}\right)\delta$$

The load distribution P_{a_δ} may be seen to be identical with the load distribution caused by changes in the angle of attack of the plain airfoil and indicates a change in ideal angle of attack equal to $\frac{1}{\pi}(\pi-\theta_0)\delta$ caused by the flap deflection δ. Glauert's expression for the lift increment (at constant angle of attack) caused by deflection of a flap is

$$c_{l_\delta}=2[(\pi-\theta_0)+\sin\theta_0]\delta$$

which may also be broken up into the components

$$c_{l_{a_\delta}}=2(\pi-\theta_0)\delta$$

and

$$c_{l_{b_\delta}}=2\sin\theta_0\delta$$

The values of the pressure-difference coefficients for uni

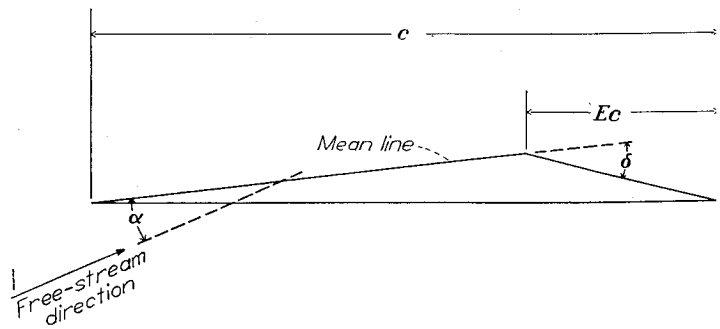

FIGURE 1.—Definition of parameters used in flap theory.

incremental lift coefficient may then be expressed as

$$\frac{P_{a_\delta}}{c_{l_{a_\delta}}}=\frac{2(1+\cos\theta)}{\pi\sin\theta}$$

and

$$\frac{P_{b_\delta}}{c_{l_{b_\delta}}}=\frac{4}{\pi\sin\theta_0}\sum_{n=1}^{\infty}\frac{\sin n\theta_0\sin n\theta}{n}$$

which may be reduced to

$$\frac{P_{b_\delta}}{c_{l_{b_\delta}}}=\frac{2}{\pi\sin\theta_0}\log_e\frac{\sin\frac{1}{2}(\theta_0+\theta)}{\sin\frac{1}{2}(\theta_0-\theta)}$$

The thin-airfoil theory indicates that these increments in load distribution will be the same regardless of the original shape of the mean line. From these equations, therefore, the theoretical incremental load distribution may be calculated for any airfoil section equipped with a plain flap.

The pitching-moment increment has been derived by Glauert as

$$\Delta c_m=-\frac{1}{2}\left(\sin\theta_0-\frac{1}{2}\sin 2\theta_0\right)\delta$$

For convenience in analysis, the pitching-moment increment caused by flap deflection is frequently expressed as a function of the lift increment caused by flap deflection. The ratio of pitching-moment increment to lift-coefficient increment provides the relation

$$\frac{\Delta c_m}{\Delta c_l}=\frac{-\frac{1}{4}\left(\sin\theta_0-\frac{1}{2}\sin 2\theta_0\right)}{(\pi-\theta_0)+\sin\theta_0}$$

This equation shows that the ratio of pitching-moment-coefficient increment caused by flap deflection to lift-coefficient increment caused by flap deflection is a constant for any given flap and is a function only of the flap-chord ratio.

The hinge moment of the flap was determined by considering only that part of the load over the flap itself and results in the equation

$$c_h=\frac{b_1}{a_1}c_l-2b\delta$$

where

$$\frac{b_1}{a_1}=\frac{1}{\pi E^2}\left[\left(\frac{3}{2}-E\right)\sqrt{E(1-E)}-\left(\frac{3}{2}-2E\right)\left(\frac{\pi}{2}-\cos^{-1}\sqrt{E}\right)\right]$$

$$b=\frac{2(1-E)\sqrt{E(1-E)}}{\pi E^2}\left[\frac{\pi}{2}-\cos^{-1}\sqrt{E}-\sqrt{E(1-E)}\right]$$

Values of b_1/a_1 and b are shown plotted against flap-chord ratio E in figure 2.

In reference 4, Pinkerton developed equations for the normal-force coefficient on a deflected flap on the basis of the thin-airfoil theory by integrating the load distribution over the flap. This integration results in an equation for the flap normal force similar to Glauert's equation for the flap hinge moment:

$$c_{n_f}=\eta_0 c_l-\eta\delta$$

where

$$\eta_0=\frac{2}{\pi(1+\cos\theta_0)}(\pi-\theta_0-\sin\theta_0)$$

$$\eta=\frac{4}{\pi(1+\cos\theta_0)}\left\{\sin^2\theta_0(1+\cos\theta_0)+2\sum_{n=2}^{\infty}\left[\frac{\sin\theta_0\sin n\theta_0\cos n\theta_0}{n^2-1}-\frac{\cos\theta_0\sin^2 n\theta_0}{n(n^2-1)}\right]\right\}$$

A general summation of the series term in the expression for η has not been found so that approximate methods of calculation have been used to calculate these values. Values of η and η_0 are shown plotted against E in figure 3.

An examination of Glauert's equations for the load distributions caused by deflection of a plain flap indicates that infinite pressures are encountered both at the leading edge and at the flap hinge. A better indication of the actual flow conditions could be obtained if the pressure distributions were caculated by the thick-airfoil theory of Theodorsen (reference 5). This process, however, is extremely laborious and breaks down just as the thin-airfoil theory does when the flow separates from the airfoil. In reference 6, a method has been derived by Allen for rapidly computing the load distribution over airfoils with flaps. This method is based on an empirical relation between the theoretical load distribution and experimentally determined values. For all flap deflections at which the flap is unstalled, a single relation was found to apply; but at higher deflections, a different relation must be used for each flap angle. In the application of this method, the load distribution is related directly to the lift-coefficient increment rather than the flap deflection which was used in Glauert's theoretical treatment. The flap deflection is important only at high deflections where it determines the shape of the empirical relation between the theoretical and experimental results. The lift-coefficient increment must be determined from force tests, and the division of the lift increment between incremental additional and incremental basic components is accomplished by the use of the experimental pitching-moment increment and empirically determined locations for the centroid of the incremental basic load.

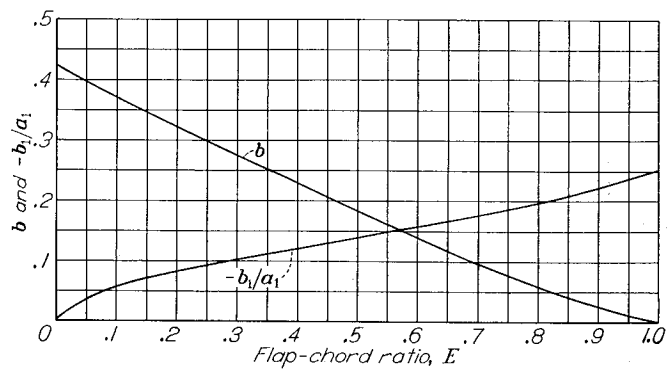

FIGURE 2.—Values of factors b and $-b_1/a_1$ in equation for hinge-moment coefficients. Reference 3.

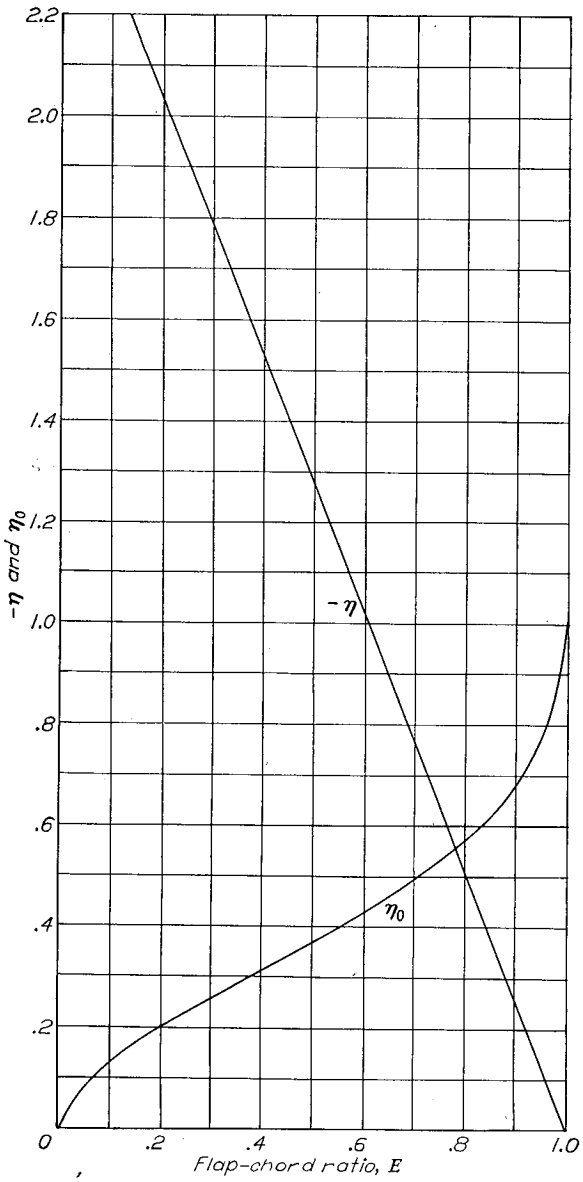

FIGURE 3.—Factors η and η_0 in equation for flap normal-force coefficients. Reference 4.

Data required for the application of this method to the determination of load distributions are the lift and the quarter-chord pitching moments at a given angle of attack for the airfoil with the flap both retracted and deflected, and the class of additional distribution to be used. The class of additional distribution to be used for conventional airfoil sections is given in reference 6 and computed additional distributions (in the form $\Delta v_a/V$, the nondimensional local increment of velocity caused by additional type of load distribution) for a number of NACA sections, both conventional and low drag, are given in reference 7. The lift and moment coefficients given are assumed equal to c_{n_1}, c_{m_1}, c_{n_2}, and c_{m_2} as shown in figures 4 (a) and 4 (b). The assumption is made that the normal force and pitching moments corresponding to the distribution of figure 4 (c) are not significantly different from those of figure 4 (a). Then (fig. 4 (d)):

$$\Delta c_m = c_{m_2} - c_{m_1}$$

$$\Delta c_n = c_{n_2} - c_{n_1}$$

These incremental coefficients are then converted to coefficients corresponding to the distribution shown in figure 4 (e) by means of the following equations:

$$\Delta c_m{}' = \tau_m \Delta c_m$$

$$\Delta c_n{}' = \Delta c_n + \tau_n \Delta c_m$$

The factors τ_n and τ_m are given in tables V and VI of reference 6. The incremental basic normal-force distribution is responsible for the entire incremental pitching-moment coefficient $\Delta c_m{}'$ and the magnitude of the incremental basic normal-force coefficient is therefore determined from the equation

$$c_{n_{b_\delta}} = \frac{\Delta c_m{}'}{G}$$

where G is equal to the distance of the centroid of the incremental basic normal-force distribution from the quarter-chord axis and is given for various flap-chord ratios and flap deflections in table IV of reference 6. The incremental additional normal-force coefficient is then equal to:

$$c_{n_{a_\delta}} = \Delta c_n{}' - c_{n_{b_\delta}}$$

The values of the pressure-difference coefficient in terms of the stream dynamic pressure q may then be obtained from

$$P_{a_\delta} = \frac{P_{a_\delta}}{c_{n_{a_\delta}}} c_{n_{a_\delta}}$$

and

$$P_{b_\delta} = \frac{P_{b_\delta}}{c_{n_{b_\delta}}} c_{n_{b_\delta}}$$

and the values of $P_{a_\delta}/c_{n_{a_\delta}}$ and $P_{b_\delta}/c_{n_{b_\delta}}$ are obtained from reference 6 or 7. It is shown in reference 6 that the values of $P_{b_\delta}/c_{n_{b_\delta}}$ and G change with a change in flap deflection whereas, the theory would indicate that these values should be independent of flap deflection for a given flap-chord ratio. These differences are caused by the fact that above a deflection of about 15° the flow begins to separate at the flap hinge. The values in the range where no separation is encountered are the same regardless of flap deflection. The value of 15° as a limit for the flap deflection where unseparated flow exists should be used with caution since a number of factors, including Reynolds number, surface condition, and leaks at the flap hinge, can have a large effect on the flap deflection at which this separation begins. Distributions are also given in reference 6 for airfoils with split flaps based on the assumption that the flow over a split flap should be the same as the flow over a plain flap with a boundary layer over the flap of thickness equal to the distance from the airfoil upper surface to the flap lower surface. The analysis reported in reference 6 showed that above a flap deflection of about 40° the load distributions for plain and split flaps were identical.

The incremental flap normal force and hinge moment caused by flap deflection are equal to the sums of the contributions to each from the incremental basic and incremental

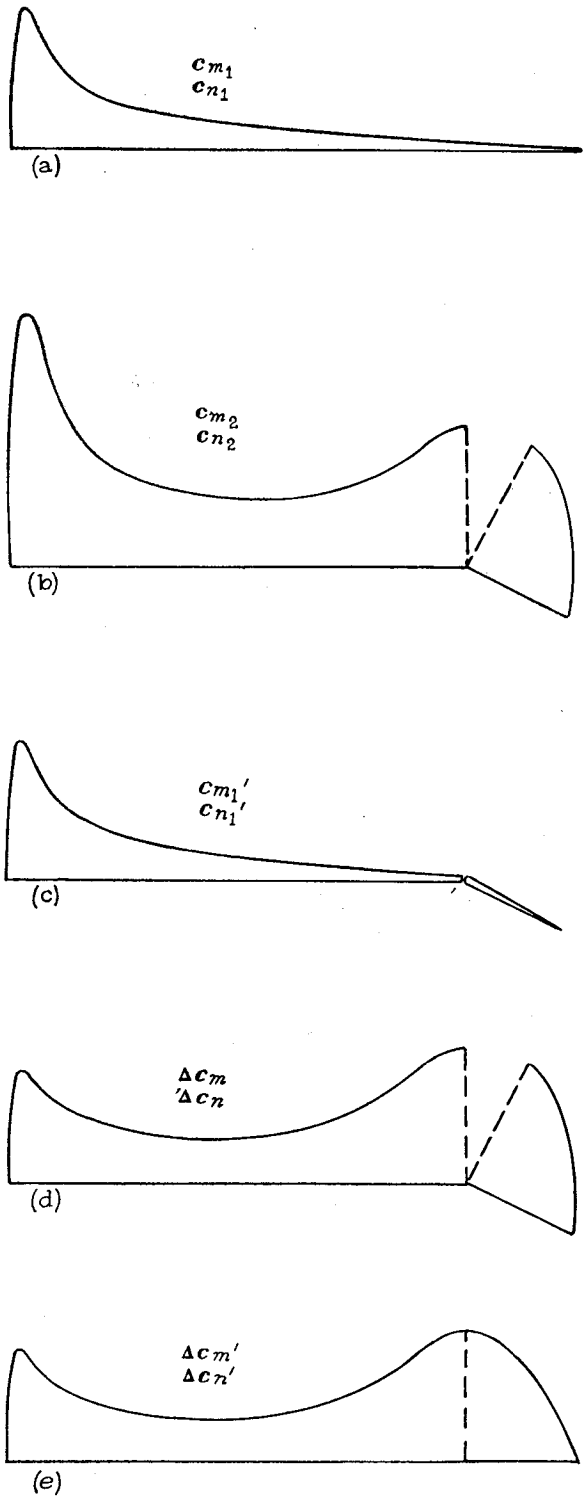

(a) Normal-force distribution for airfoil with flap neutral.
(b) Normal-force distribution for airfoil with flap deflected.
(c) Distribution shown in (a) with flap normal-force distribution plotted normal to flap-deflected chord.
(d) Incremental normal-force distribution caused by flap deflection.
(e) Distribution shown in (d) plotted normal to flap-neutral chord.

FIGURE 4.—Normal-force distribution and incremental normal-force distribution for flaps neutral and deflected.

additional normal-force distributions. The flap normal-force coefficient and flap hinge-moment coefficient are equal to:

$$c_{n_{f_\delta}}=\gamma_{a_\delta}c_{n_{a_\delta}}+\gamma_{b_\delta}c_{n_{b_\delta}}$$

$$c_{h_{f_\delta}}=\eta_{a_\delta}c_{n_{a_\delta}}+\eta_{b_\delta}c_{n_{b_\delta}}$$

The values of the factors γ and η are given in reference 6.

Comparisons of experimental data with loads and distributions calculated by this method show that excellent agreement is obtained for plain flaps when the proper assumption is made as to whether the flap is stalled. Similar comparisons made for split flaps show that, although the over-all effects of the flap are shown quite well over the forward part of the airfoil, rather large discrepancies are noted over the rear with the result that loads and moments predicted in this manner are not accurate.

By using the assumption that a slotted flap is merely a plain flap with a boundary-layer control slot and by considering the chord to be equal to the total chord of the wing with flap extended, some comparisons have been made for slotted flaps. These comparisons show again that the over-all effect is predicted to an accuracy suitable for wing structural purposes but with large differences near the flap where flow through the slot can affect the load distribution. The flap loads for slotted flaps are indicated with only qualitative accuracy.

DISCUSSION OF EXPERIMENTAL RESULTS

PLAIN FLAPS

The plain flap is one of the simplest lift-increasing devices in use, consisting merely of a hinged part of the wing near the trailing edge which can be deflected downward to increase the camber and, therefore, the lift. The only fundamental design parameters (aside from airfoil section and Reynolds number) which can have an effect on the performance of a plain flap are the flap-chord ratio and the angle to which the flap is deflected.

MAXIMUM LIFT

Curves of maximum lift coefficient are shown plotted against flap deflection for various sizes of plain flaps on several airfoil sections in figure 5 (data from references 7 to 12). Generally, the maximum lift coefficient is shown to increase with flap deflection to a maximum at a flap deflection of about 60° or 70° except for the largest flap (0.60c) which increases the maximum lift coefficient only for very small deflections.

A comparison of the increments in maximum lift coefficient for the NACA 23012 airfoil with 0.20c flaps at Reynolds numbers of 0.609×10^6 and 3.5×10^6 shown in figure 6 indicates that, in this range of Reynolds number at least, the maximum-lift-coefficient increment is essentially independent of scale. Optimum maximum-lift-coefficient increments (the highest maximum-lift-coefficient increments attained) are plotted against flap-chord ratio for the three NACA 230-series and the Clark Y airfoils in figure 7 on the basis of the rather meager data available. These data show that the best maximum lift coefficients are attained with flaps of 0.20c or 0.25c and that the maximum-lift-coefficient increment increases with airfoil thickness ratio for the NACA 230-series airfoils in the range of thicknesses shown. The data for the NACA 66(215)–216 (fig. 5) airfoil seem to agree with the increment for an NACA 230-series airfoil of

similar thickness; and although the NACA 65,3–618 airfoil shows lower increments, the value of the highest maximum lift coefficient for this airfoil is nearly as high as that of the NACA 66(215)–216 airfoil.

A gap between the airfoil and flap at the flap hinge allows air to leak through from the high pressure on the lower surface to the low pressure on the upper surface and to decrease the effectiveness of the flap. Maximum-lift data from reference 10 are shown in figure 8 for an airfoil with a 0.20c plain flap with a 0.0032c gap both sealed and unsealed. The maximum lift coefficients are higher in all cases with the gap sealed, and the decrement in maximum lift coefficient caused by the gap increases as the flap deflection is increased.

DRAG

The effect of flap size on the drag coefficients of airfoils equipped with plain flaps is shown in figure 9. Envelope polars of total-wing drag coefficient are shown for a Clark Y wing of aspect ratio 6 equipped with 0.10c, 0.20c, and 0.30c full-span plain flaps. These data indicate an increase in drag coefficient with flap size at any lift coefficient above about 1.2. A large part of the drag of airfoils equipped with deflected plain flaps is caused by the fact that the flow over the flap separates at relatively low deflections (of the order of 15° or 20°). The higher drags of the larger flaps are therefore probably a result of a larger separated area and a larger wake

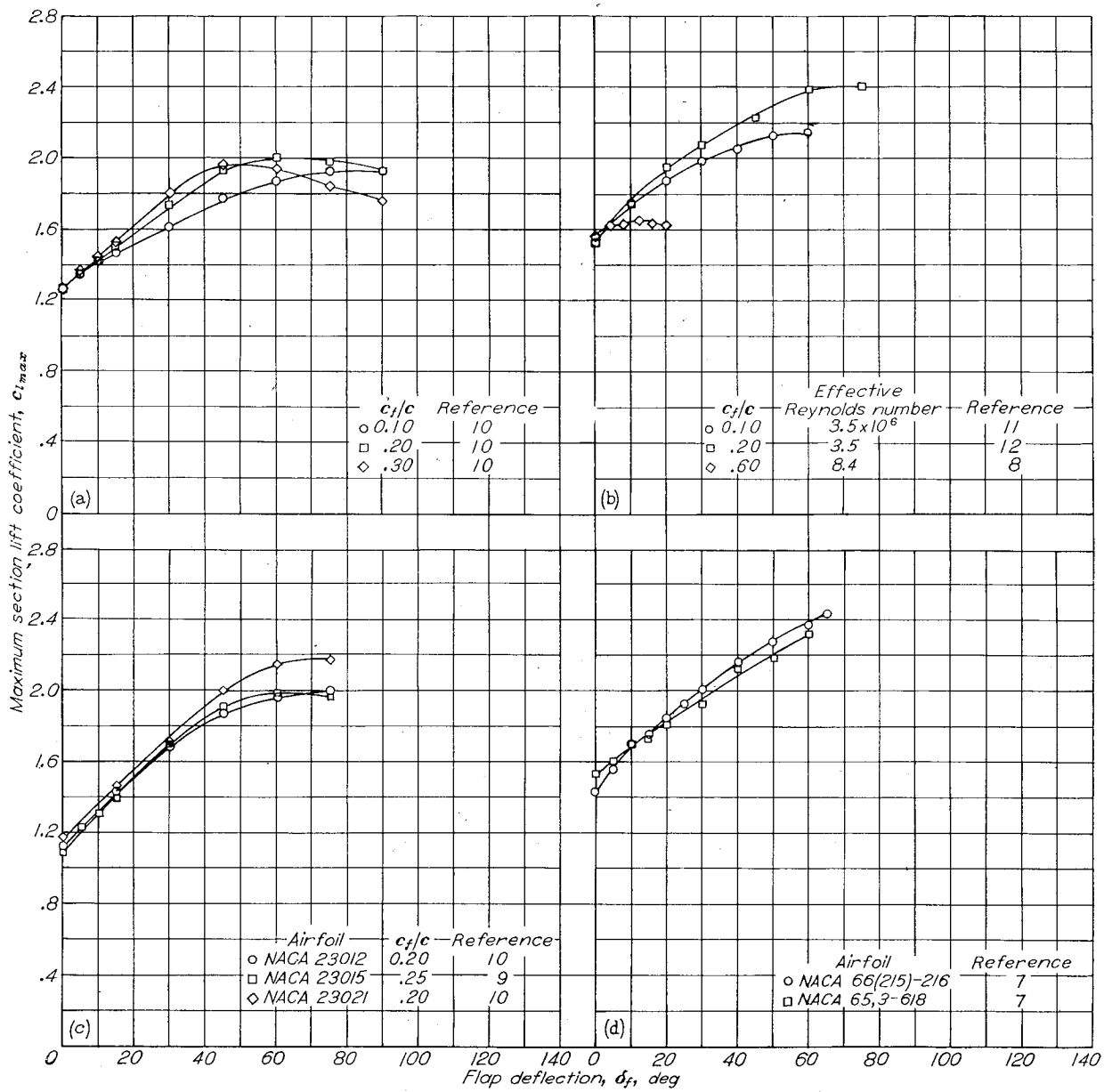

(a) Clark Y airfoil; $R=0.609\times10^6$.

(b) NACA 23012 airfoil.

(c) NACA 230-series airfoils; $R=0.609\times10^6$.

(d) NACA 6-series airfoils; $R=6.0\times10^6$, $\frac{c_f}{c}=0.20$.

FIGURE 5.—Variation of maximum section lift coefficient with flap deflection for several airfoil sections equipped with plain flaps.

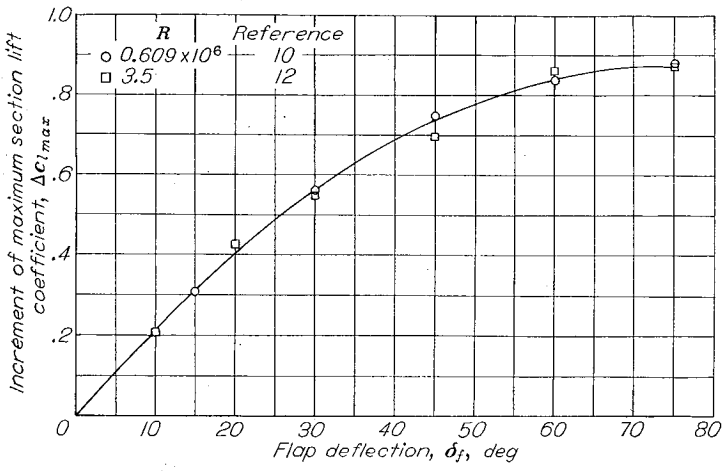

FIGURE 6.—Effect of Reynolds number on increment of maximum section lift coefficient caused by deflection of a 0.20c plain flap on the NACA 23012 airfoil section.

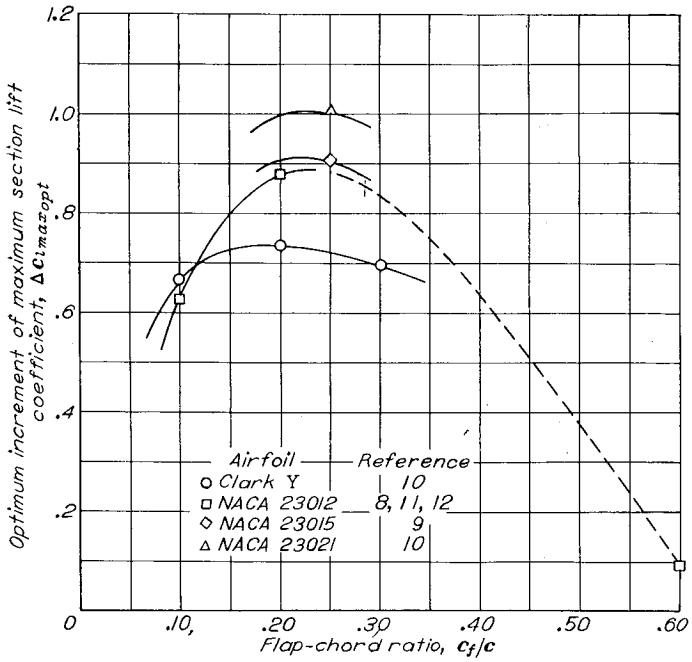

FIGURE 7.—Variation of optimum increment of maximum section lift coefficient with flap-chord ratio for several airfoil sections equipped with plain flaps.

Drag data on an NACA 23012 airfoil fitted with a 0.20c flap are shown in figure 10 at two values of the Reynolds number (references 12 and 13). These data show that the favorable effect of increasing Reynolds numbers extends throughout the entire range of lift coefficient. It should be noted that the effective Reynolds number of 8.4×10^6 given in figure 10 corresponds to a test Reynolds number of approximately 3×10^6. Any conclusion concerning the effect of Reynolds number based on these data is subject to the limitations of the concept of effective Reynolds number.

Drag polars for several low-drag airfoils equipped with plain flaps are shown in reference 7. These data show that the low-drag range of smooth low-drag airfoils can be shifted to higher lift coefficients by small deflections of a plain flap. It is obvious therefore that it should be possible to use a flap of this type to maintain low profile drags through a wide range of lift coefficient.

864781—50——2

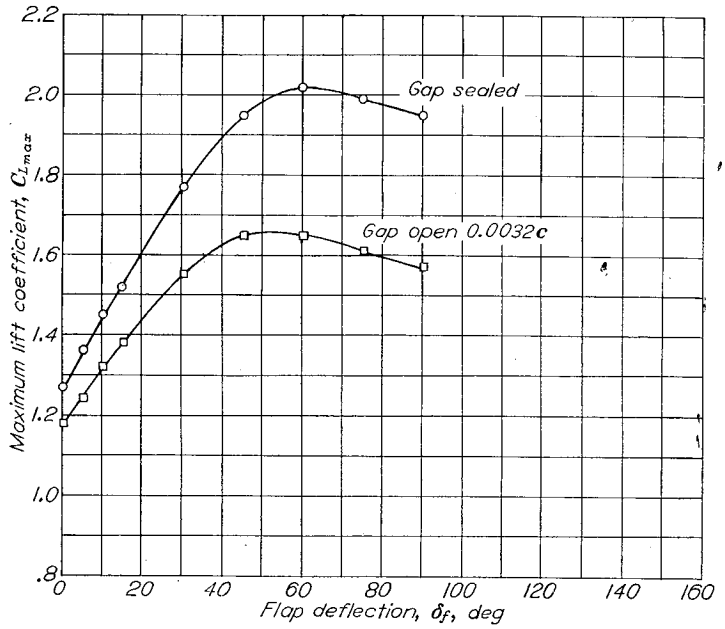

FIGURE 8.—Effect of gap seal on maximum lift coefficient of a rectangular Clark Y wing equipped with a full-span 0.20c plain flap. $A=6$; $R=0.609\times10^6$; reference 10.

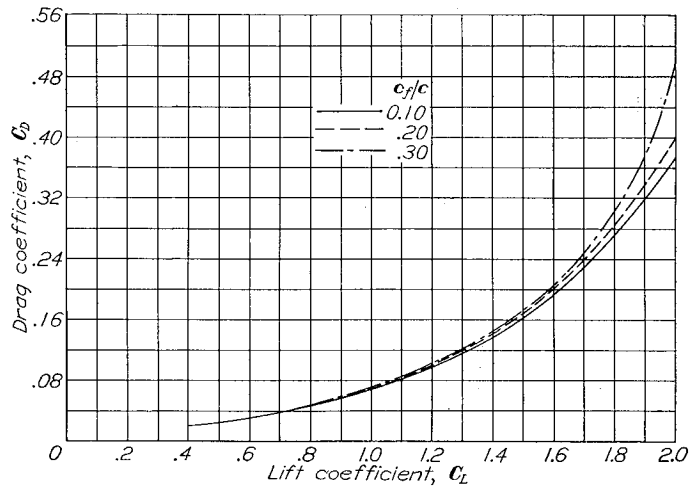

FIGURE 9.—Envelope drag polars for a Clark Y airfoil equipped with plain flaps of various sizes. $R=0.609\times10^6$; $A=6$; reference 10.

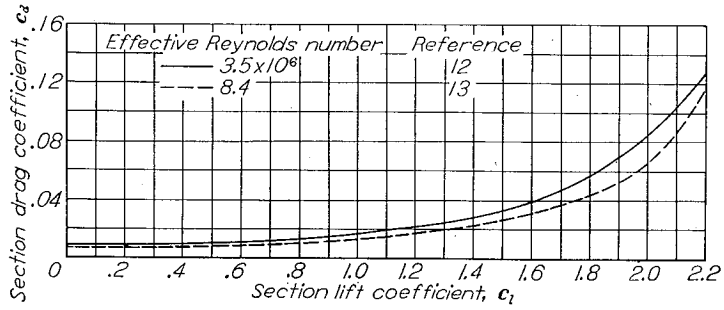

FIGURE 10.—Envelope drag polars for an NACA 23012 airfoil equipped with a 0.20c plain flap at two Reynolds numbers.

PITCHING MOMENT

The ratio of pitching-moment increment to lift increment caused by deflection of a plain flap has been shown by Glauert to be a constant for any given flap and to be dependent only on flap-chord ratio. Experimental data indicate that this linear relation of pitching moment to lift is actually obtained. Figure 11 shows a curve of the theoretical slope $\Delta c_m/\Delta c_l$ plotted against flap-chord ratio along with several experimental values. The agreement is shown to be reasonably good.

FLAP LOADS AND MOMENTS

The method derived by Allen for predicting flap loads and moments has been summarized in the section on flap theory. Flap normal forces, taken from reference 14, at an angle of attack of 0° are shown in figure 12 along with the normal forces calculated by Allen's method. These results show very good agreement between calculated and experimental results. Similar comparisons between experimental flap loads and loads calculated by means of the thin-airfoil theory show great discrepancies. The large errors resulting from the use of the thin-airfoil theory can probably be ascribed to the fact that the thin-airfoil theory bases all results merely on the flap deflection. Because of separation of the flow from the airfoil surface, flap deflection is not so effective for increasing the loads on the wing as would be indicated by the perfect-fluid theory.

Hinge moments for plain flaps are subject to the same differences between the ideal conditions and those normally encountered in practice. The same sort of comparison could therefore be expected between the theory and experiment. Data are shown in figure 13 for the 0.20c flap on the NACA 23012 airfoil and again show good agreement with predictions based on Allen's empirical method.

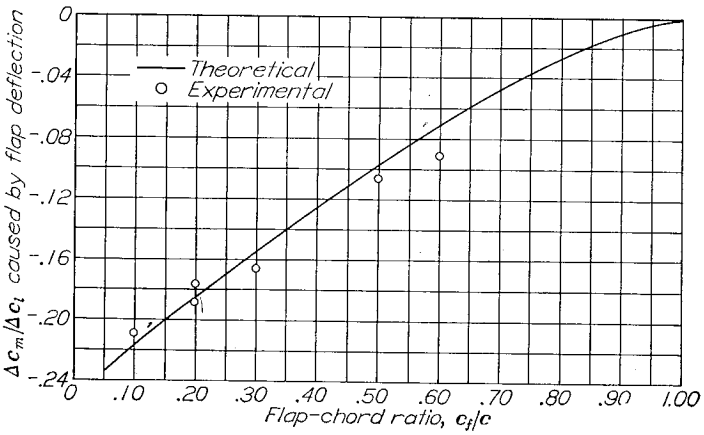

FIGURE 11.—Variation of ratio of pitching-moment coefficient to lift coefficient at constant angle of attack with flap-chord ratio.

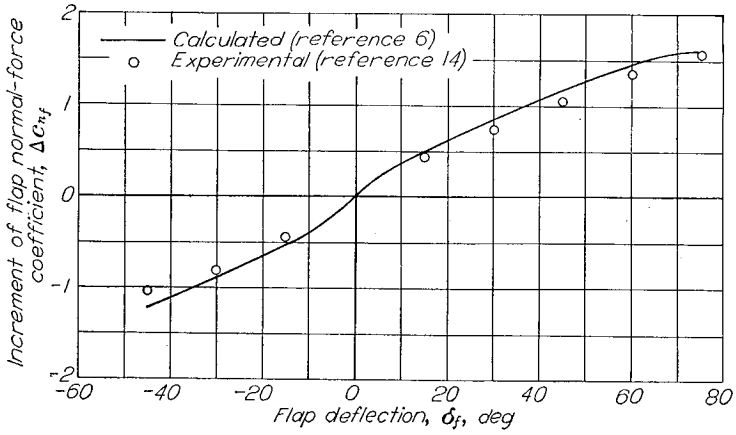

FIGURE 12.—Variation of flap normal-force coefficient with flap deflection. NACA 23012 airfoil; 0.20c plain flap; $\alpha_0=0°$.

SUMMARY OF PLAIN-FLAP DATA

Maximum lift coefficients for airfoils with plain flaps are shown to increase with flap-chord ratio to a maximum at a flap-chord ratio of about 0.20c to 0.25c. The highest maximum lift coefficients for airfoils with flaps of about this size usually occur at flap deflections of about 60°. Within a range of Reynolds number from 0.6×10^6 to 3.5×10^6 at least, scale seems to have little effect on maximum-lift-coefficient increments caused by deflection of a plain flap. Rather meager data for NACA 230-series airfoils show that the highest maximum-lift-coefficient increment attainable with plain flaps of a given size increases as the airfoil thickness is increased. Drag coefficients are shown to increase appreciably with flap size for all lift coefficients above about 1.2, and available data indicate that favorable scale effects are obtained throughout the complete range of lift coefficient. The increment of pitching-moment coefficient caused by flap deflection is a linear function of the increment of lift coefficient, and the ratio of pitching moment to lift agrees reasonably well with the thin-airfoil theory. Flap normal forces and hinge moments may be predicted with good accuracy by the method derived by Allen in reference 6.

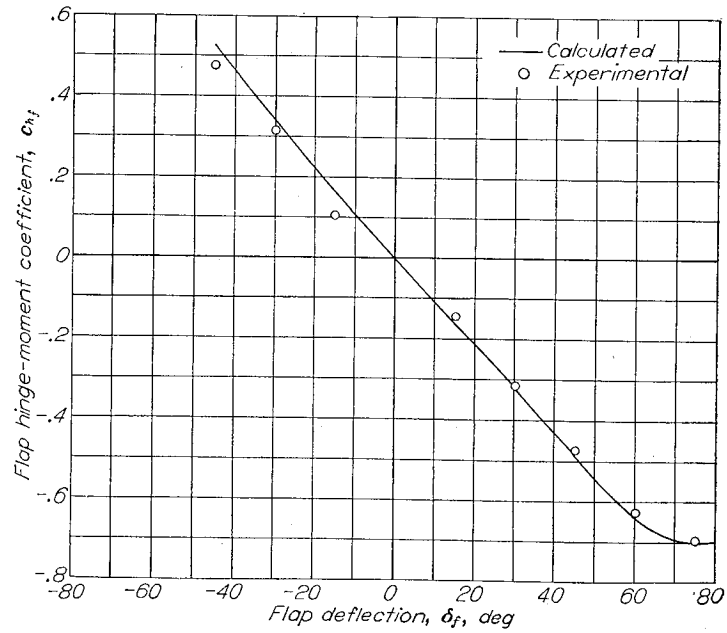

FIGURE 13.—Variation of flap hinge-moment coefficient with flap deflection. NACA 23012 airfoil; 0.20c plain flap; $\alpha_0=0°$.

SPLIT FLAPS

A split flap is similar to a plain flap in that it is formed merely by a hinged part of the wing near the trailing edge. For a split flap, however, only the lower part of the wing is hinged, the upper surface remaining in place. The increase in lift caused by deflection of a split flap is a result of an increase in the effective camber of the airfoil section just as is the case for plain flaps. The important design parameters which will affect the aerodynamic characteristics of a wing section with a split flap are, therefore, the flap-chord ratio and the flap deflection.

MAXIMUM LIFT

The effect of flap deflection on the maximum lift coefficients of NACA 23012, 23021, and 23030 airfoil sections with split flaps ranging in size from 0.10c to 0.40c are shown in figure 14 (data from reference 15) and optimum increments in maximum lift coefficient are shown plotted against flap-chord ratio in figure 15. Although the increments of maximum lift coefficient are considerably higher for thick than for thin sections, the values of maximum lift coefficient vary in a different manner with thickness because of the decrease in maximum lift coefficient of the airfoil with flap undeflected as the thickness is increased. These data show that as the airfoil thickness is increased increments of maximum lift coefficients, flap deflections for maximum lift, and the size of flap that provides the highest increment of maximum lift coefficient also increase. For any given airfoil section the flap deflection at which the highest maximum lift coefficient was measured decreased as the size of flap was increased. A comparison of the data in figure 14 with the data shown previously for plain flaps (fig. 5) of similar size shows that higher maximum lift coefficients are obtained for airfoils with split flaps than with plain flaps and that the optimum maximum lift coefficients are obtained at higher flap deflections and higher flap-chord ratios. The reason for the higher maximum lift coefficients obtained with split flaps can probably be attributed to the fact that the upper surface of the wing is not disturbed and the flow is not required to follow an abrupt downward curvature over the flap. The flow over the flapped part of the airfoil, therefore, has a tendency to remain unstalled up to higher flap deflections and higher flap-chord ratios for split flaps than for plain flaps. Maximum-lift data from reference 16 are shown in figure 16 for three NACA 6-series airfoil sections equipped with 0.20c split flaps. These data indicate the same tendency toward higher optimum deflections for thicker airfoils as was shown by the NACA 230-series sections.

In order to provide a simple means for showing the effect of flaps on airfoil section characteristics, all the airfoils tested in connection with the low-drag airfoil program (reference 7) have been tested with 0.20c split flaps deflected 60°. With some types of flap (particularly slotted) a change in airfoil shape also changes the shape of the flap that may be fitted into the available space and, therefore, changes the characteristics of the airfoil-flap combination. The systematic split-flap data should be useful, however, for showing the manner in which airfoil parameters alone affect the characteristics of airfoils with flaps.

The effects of thickness ratio and camber on maximum lift coefficients of NACA 64-series airfoil sections with and without 60° split flaps are shown in figure 17 (data from reference 7). These data show that, although the maximum lift coefficients of the plain airfoil sections decrease as the

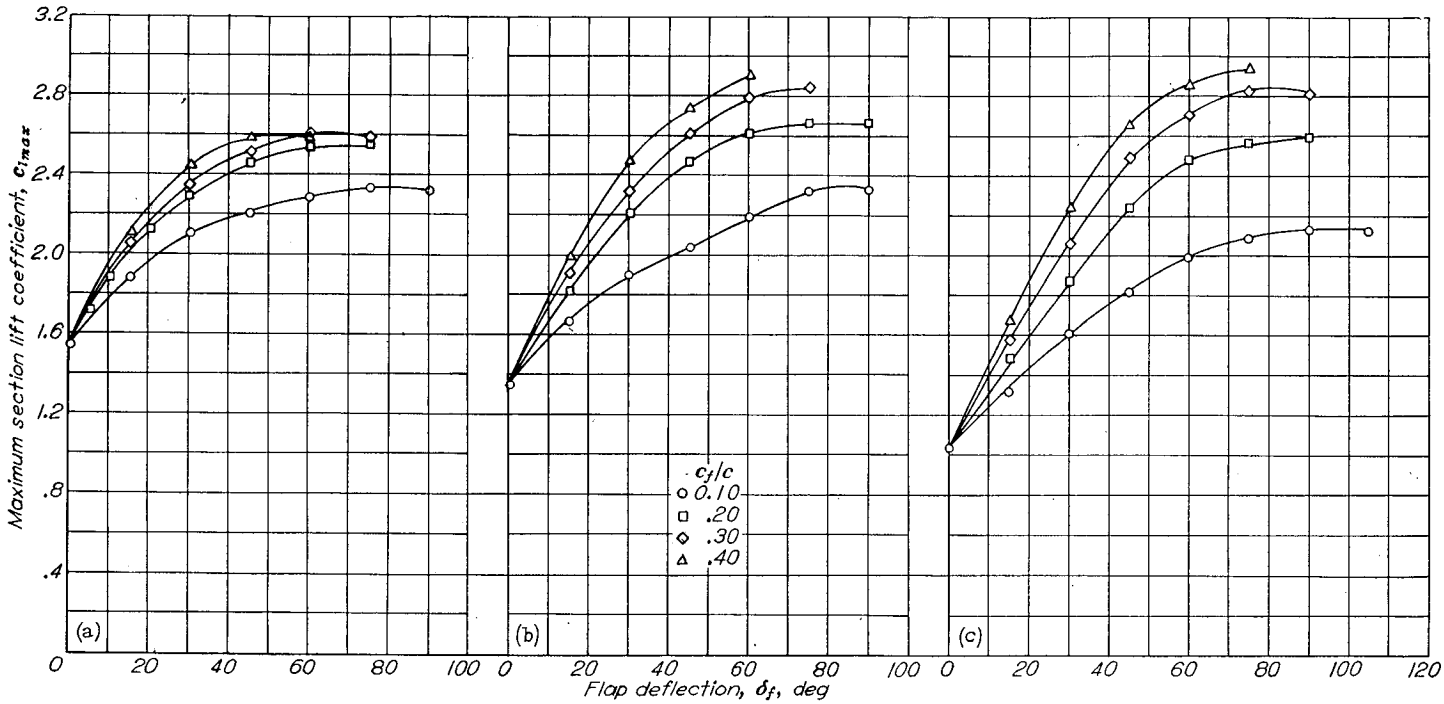

(a) NACA 23012 airfoil section. (b) NACA 23021 airfoil section. (c) NACA 23030 airfoil section.

FIGURE 14.—Variation of maximum section lift coefficient with flap deflection for three NACA 230-series airfoils equipped with split flaps of various sizes. R=3.5×10^6; reference 15.

thickness ratio is increased above approximately 0.12, the maximum lift coefficients of the flapped airfoils continue to increase to thickness ratios of at least 0.18. Increases in design lift coefficient are shown to increase maximum lift coefficients of both the plain and the flapped airfoils by an equal amount for airfoils of low and moderate thicknesses. At the higher thicknesses, however, the effect of increasing camber is smaller and for the 21-percent-thick airfoils is actually to decrease the maximum lift coefficients with flaps deflected. Maximum lift coefficients for NACA 23012 and NACA 23015 airfoil sections are also shown in this figure. The maximum lift coefficients for the NACA 230-series sections are shown to follow the same trend as the NACA 6-series sections. The variation of maximum lift coefficients with position of minimum pressure for NACA 6-series sections is shown in figure 18. In most cases these data indicate a small decrease in maximum lift coefficients of both the plain and flapped airfoils regardless of thickness ratio as the position of minimum pressure is moved to the rear.

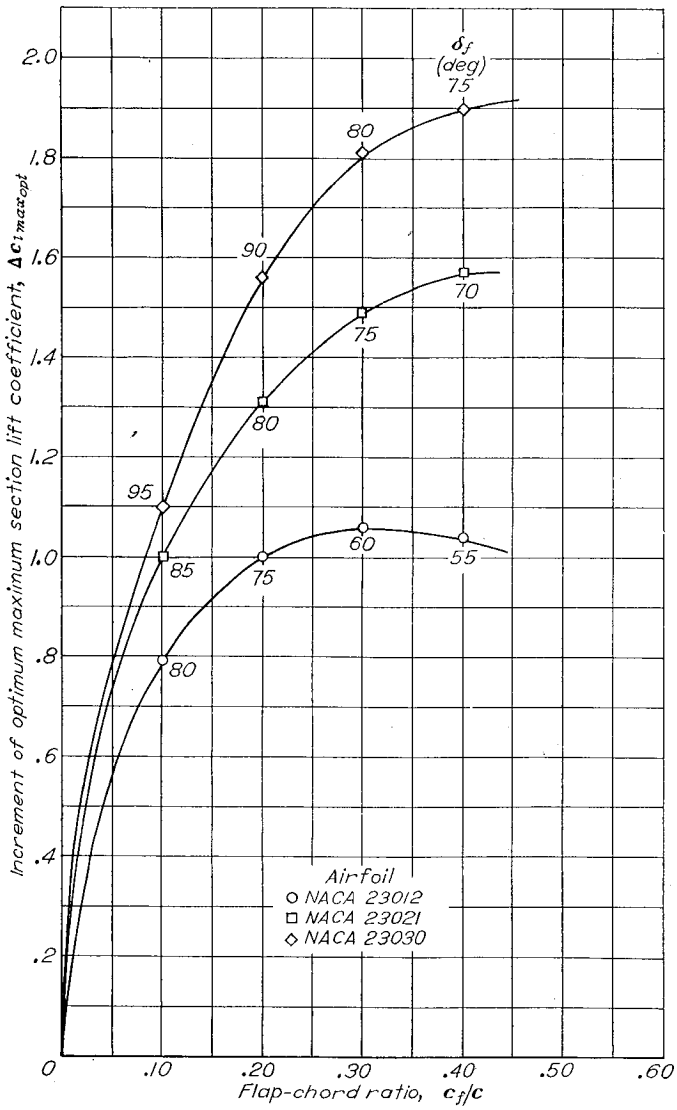

FIGURE 15.—Variation of increment of optimum maximum section lift coefficient with flap-chord ratio. NACA 230-series airfoils equipped with split flaps. $R=3.5\times10^6$.

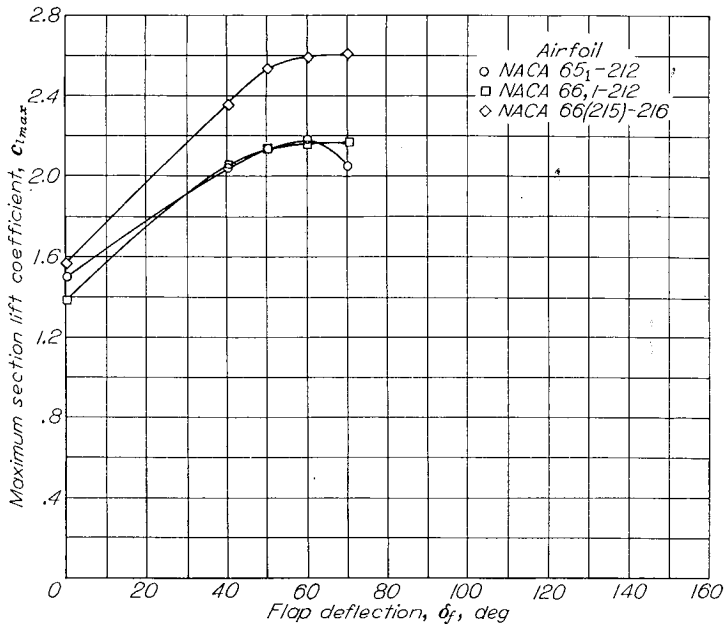

FIGURE 16.—Variation of maximum section lift coefficient with flap deflection for several NACA 6-series airfoil sections equipped with 0.20c split flaps. $R=6.0\times10^6$; reference 16.

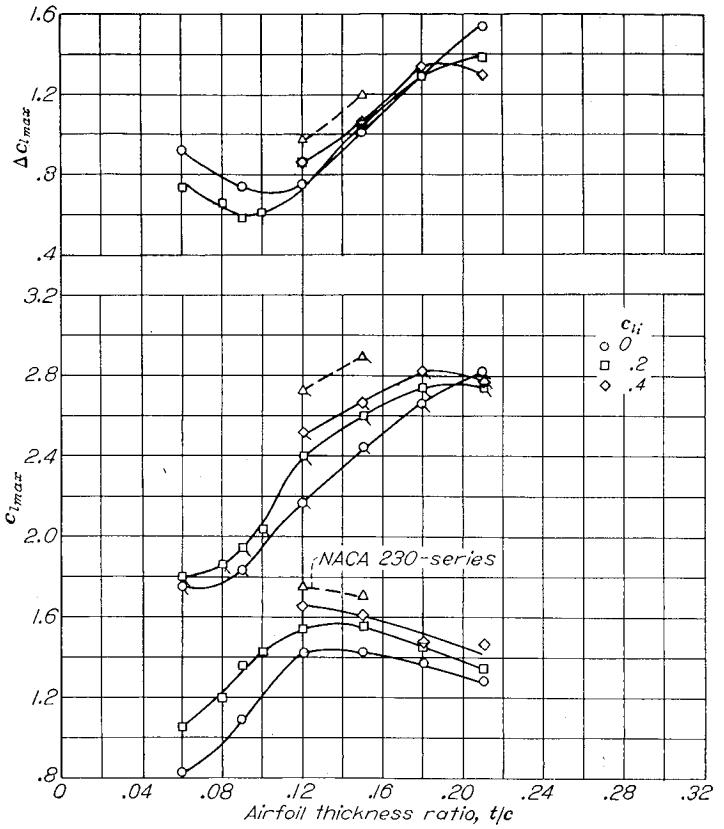

FIGURE 17.—Variation of maximum section lift coefficient with airfoil thickness ratio and camber for some NACA 64-series airfoil sections with and without simulated split flaps. $R=6.0\times10^6$; reference 7. (Flagged symbols are for 60° simulated split flap.)

The fact that all of the flap data shown in figures 17 and 18 were obtained with 0.20c flaps deflected 60° prevents a complete indication of the effects of airfoil section on maximum lift coefficient since both the optimum flap size and optimum deflection change with changes in airfoil thicknesses as shown in figure 15. This fact is particularly true

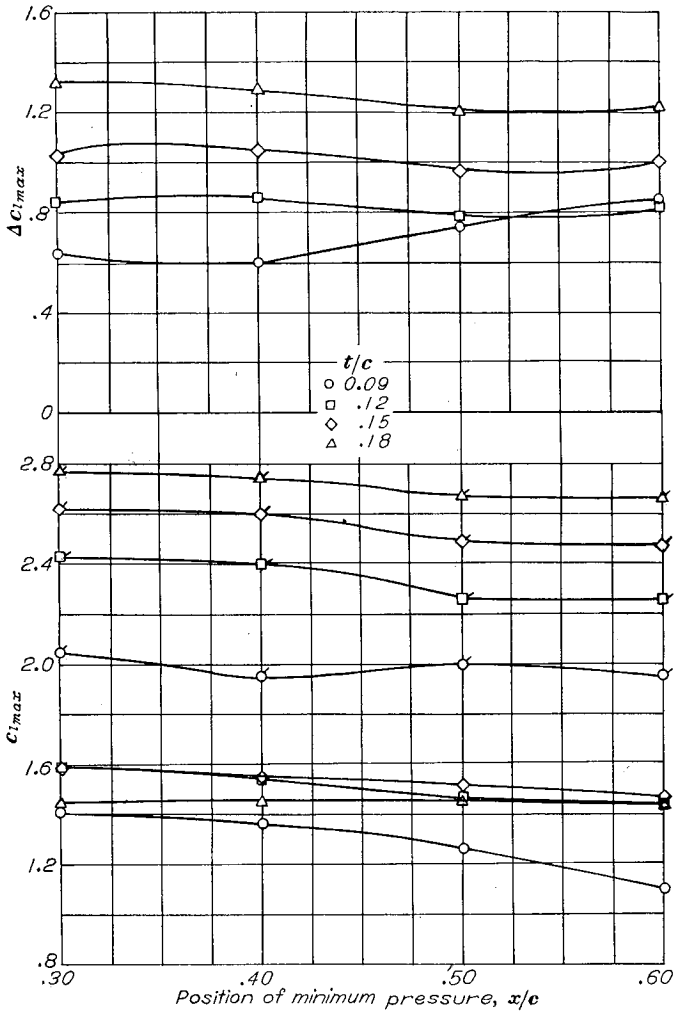

FIGURE 18.—Variation of maximum section lift coefficient with position of minimum pressure and airfoil thickness ratio for some NACA 6-series airfoil sections with and without split flaps. $c_{l_i}=0.2$; $R=6.0\times10^6$. (Flagged symbols are for 60° simulated split flap.)

of the data shown in figure 17 since both the flap-chord ratio and flap deflection for highest maximum lift coefficient increase as the airfoil thickness ratio is increased. The optimum maximum lift coefficients should, therefore, increase even more rapidly with thickness ratio than the maximum lift coefficients shown.

Data are shown in figure 19 on the effects of Reynolds number variation on the maximum lift coefficients of several NACA airfoil sections. Throughout the range of Reynolds number shown, maximum lift coefficients of both the plain and flapped airfoils in the smooth condition increase as the Reynolds number is increased, but not by a constant amount nor in any apparently predictable manner. The effects of scale on the maximum lift coefficients of NACA 6-series sections seem to be similar to those of conventional NACA 230-series sections.

The effect of Reynolds number on the maximum lift coefficients of several NACA airfoils with standard leading-edge roughness and split flaps is also shown in figure 19. The effect of Reynolds number in increasing the maximum lift coefficients of these airfoils is decreased by the addition of standard roughness and seems to be approximately the same for each of the airfoils for which data are shown. A comparison of the data for smooth and rough airfoils in figure 19 shows that the decrease in maximum lift coefficients of airfoils with split flaps increases as the Reynolds number is increased and that the effect of roughness on the maximum lift coefficients of NACA 230-series sections is greater than that on NACA 6-series sections but not enough to make the actual values of the maximum lift coefficients lower.

DRAG

Envelope drag polars for an NACA 23012 airfoil equipped with various sizes of split flaps are shown in figure 20. These data indicate that the drag coefficients of airfoils equipped with split flaps increase as the flap size is increased. These higher drags are probably caused by the increased size of the wake behind larger flaps, as is the case for plain flaps.

Envelope drag polars shown in reference 15 for flaps of various sizes on NACA 23012, 23021, and 23030 airfoils show that the drags of thicker airfoils with split flaps deflected are higher than those of thinner airfoils except in cases where the thinner airfoils tend to stall at lower lift coefficients than the thick sections.

PITCHING MOMENT

The ratio of pitching-moment increment to lift-coefficient increment caused by deflection of split flaps of various sizes on several NACA 230-series airfoil sections is shown in figure 21 (data from reference 15). These data show that the pitching moments of airfoils with split flaps do not agree with the theory as well as those with plain flaps but that the general order of magnitude of the pitching moments and the manner of variation with flap-chord ratio agree fairly well with the theory. This discrepancy may be explained by the fact that the rear part of an airfoil with a split flap deflected presents a very thick, blunt body rather than the thin mean line which is assumed in the theory and which is at least approximated by plain flaps.

FLAP LOADS AND MOMENTS

The methods for predicting flap loads and moments which are based on the thin-airfoil theory could not be expected to provide a good indication of split-flap loads since the pressure difference across the flap is not, in this case, equal to the pressure difference across the whole airfoil or, as the theory assumes, across the mean line. A comparison of some split-flap load data with loads predicted by the method given in reference 6 and described in the section on flap theory shows that, although fair agreement can be obtained at low flap deflections, the predicted values are considerably higher than the experimental results at high deflections. Pressure distributions and flap force and hinge-moment characteristics for a 0.20c split flap on the NACA 23021 airfoil are shown in reference 17.

EXTENSIBLE SPLIT FLAPS

An extensible split flap is a split flap provided with a movable hinge which is moved to the rear as the flap is deflected.

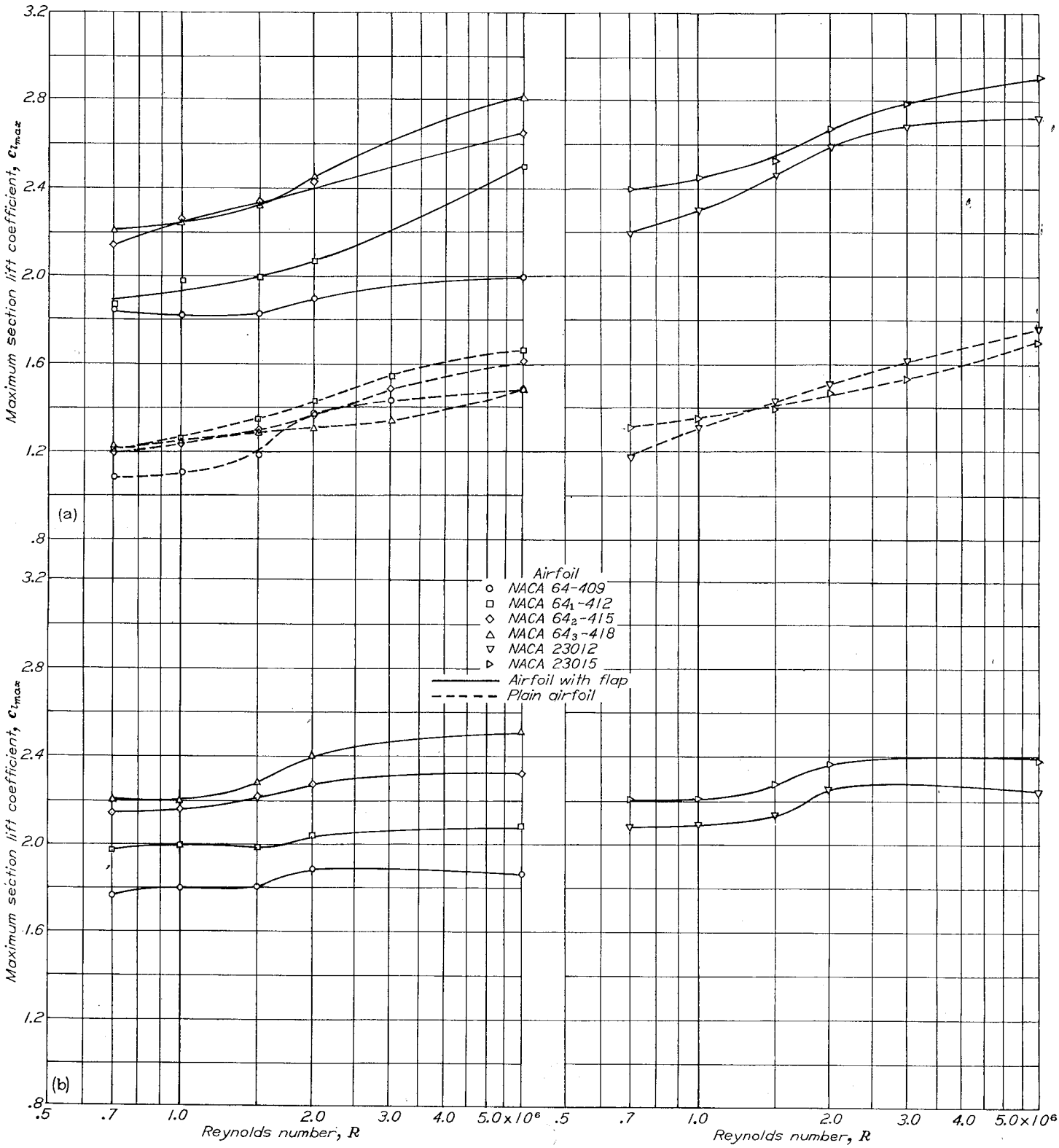

(a) Smooth airfoil.
(b) Airfoil with leading-edge roughness.

FIGURE 19.—Variation of maximum section lift coefficient with Reynolds number for several NACA airfoil sections with and without 0.20c split flaps deflected 60°.

The purpose of displacing the hinge is to provide a larger area and, therefore, greater lifts. Maximum lift coefficients taken from reference 18 are shown in figure 22 for a Clark Y airfoil equipped with split flaps of 0.20c, 0.30c, and 0.40c hinged at various positions from the normal hinge position to the trailing edge. Sizable increases in maximum lift coefficient (as high as 0.3 for the 0.40c flap) are produced by the extension of the chord in this way, increases being noted for the 0.20c flap for each extension of the flap hinge from the normal hinge axis to the trailing edge although the larger flaps produced increases for extensions of the flap hinge only to 0.90c.

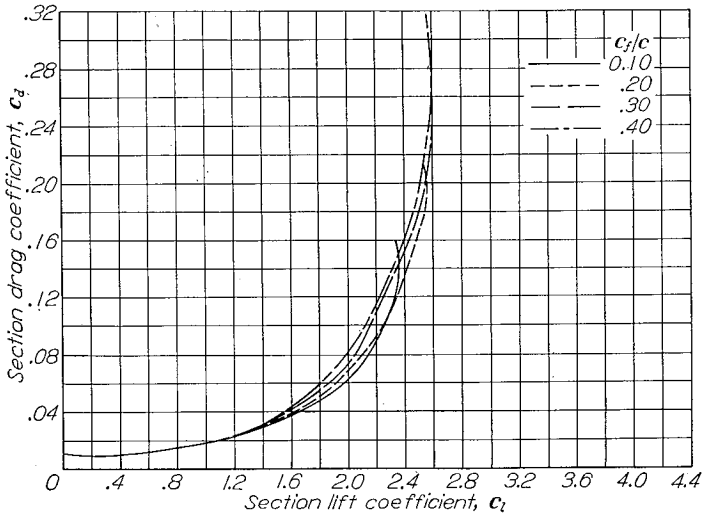

FIGURE 20.—Envelope drag polars for an NACA 23012 airfoil equipped with split flaps of various sizes. $R=3.5\times10^6$; reference 15.

Because of the fact that the extensible split flap is extended to the rear as it is deflected, the effective area of the wing behind the normal quarter-chord point is increased and the negative pitching moments become larger. Data are shown in figure 23 (from reference 18) on the effect of split-flap extension on the pitching-moment-coefficient increments caused

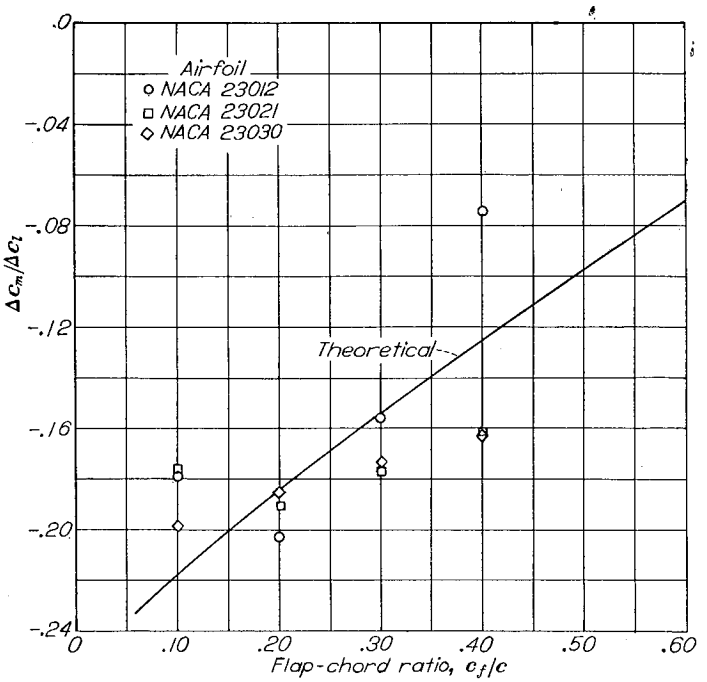

FIGURE 21.—Variation of ratio of increment of section pitching-moment coefficient to increment of section lift coefficient with flap-chord ratio for several airfoil sections equipped with split flaps. $\alpha_0=0°$; reference 15.

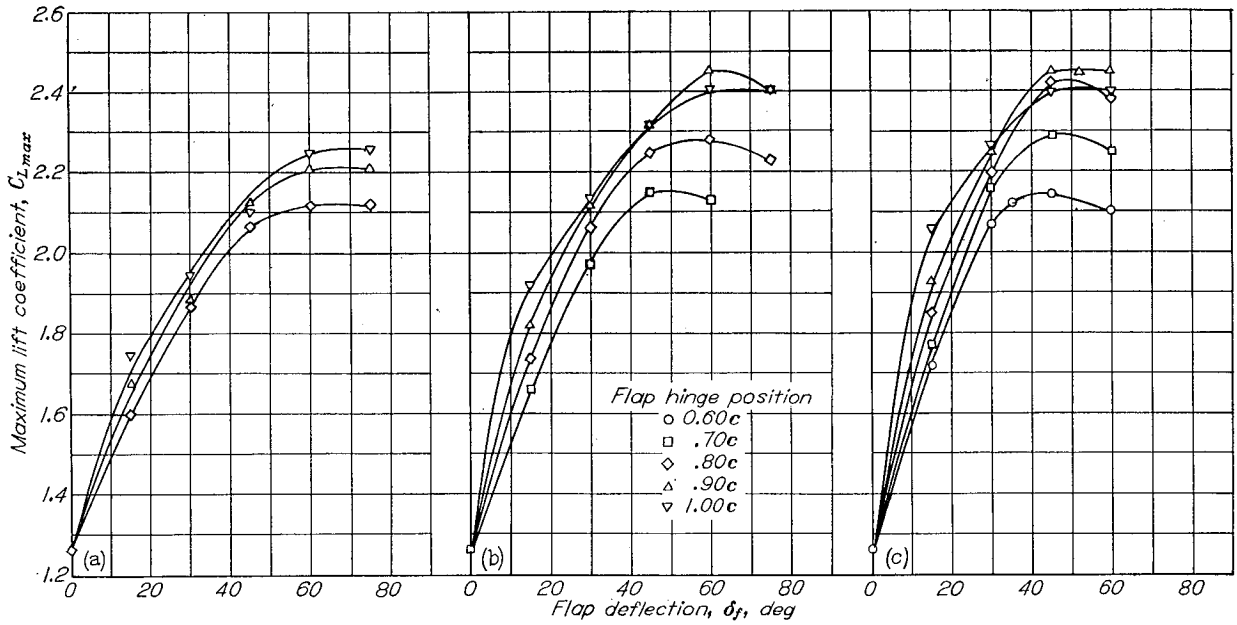

(a) $\frac{c_f}{c}=0.20$. (b) $\frac{c_f}{c}=0.30$. (c) $\frac{c_f}{c}=0.40$.

FIGURE 22.—Variation of maximum lift coefficient with flap deflection and hinge position for a Clark Y airfoil equipped with extensible split flaps of various sizes. $R=0.6\times10^6$; $A=6$; reference 18.

by deflection of the flap. The increment in pitching-moment coefficient is shown to be a linear function of the increment in lift coefficient, and the slope of the curve $\Delta c_m/\Delta c_l$ is shown to increase as the flap hinge is moved to the rear.

SUMMARY OF SPLIT-FLAP DATA

Split flaps are shown to provide higher maximum lift coefficients than plain flaps. Maximum lift coefficients, flap deflections for maximum lift, and best flap size increase as the airfoil thickness ratio is increased. Larger flaps showed higher maximum lift coefficients than smaller flaps; the highest maximum lift coefficients were obtained at lower flap deflections with the larger flaps than with the smaller flaps. Maximum lift coefficients of NACA 6-series sections with 60°, 0.20c flaps are shown to increase with airfoil thickness ratio up to thickness ratios of about 0.18c. Increase of camber increases maximum lift coefficients of thin airfoils, but this effect decreases as the airfoil thickness is increased. Leading-edge roughness has been shown to decrease the favorable scale effect on maximum lift coefficients of airfoils with split flaps. Increases in flap size or airfoil thickness ratio show increases in drag coefficients of airfoils with flaps deflected. Pitching-moment increments of airfoils with split flaps are of the same order of magnitude as shown by the thin-airfoil theory, but the agreement with the theory is not so good as that shown by the plain flaps. Displacing a split flap to the rear as it is deflected increases both maximum lift coefficients and pitching moments.

SLOTTED FLAPS

Slotted flaps are roughly similar to plain or split flaps insofar as they increase the lift of an airfoil by an increase in camber and in some cases by an increase in the chord. The slotted flap, however, is provided with a slot which delays the tendency of the flow to separate from the flap by ducting high-energy air from the lower surface and utilizing it for boundry-layer control on the flap upper surface. Deflection of slotted flaps may be obtained either by pure rotation about a fixed hinge or by a combination of translation and rotation. Slotted flaps in general use may be divided into two general classes based merely on the number of slots. Single slotted flaps are, as the name suggests, flaps which are attached to the main portion of the wing in such a manner as to provide a slot forward of the flap when the flap is deflected. Double slotted flaps are provided with a vane forward of the flap so that a double slot is formed when the flap is deflected.

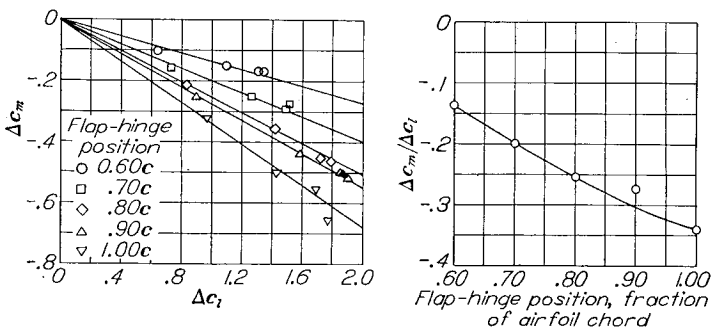

FIGURE 23.—Variation of increment of pitching-moment coefficient with increment of lift coefficient for various hinge positions of a 0.40c extensible split flap on a Clark Y airfoil. α_0=0°; reference 18.

SINGLE SLOTTED FLAPS

A typical single-slotted-flap configuration is shown in figure 24. The part of the wing upper surface which extends over the flap when retracted is called the slot lip. The effective increase in chord provided by some slotted flaps is obtained by the use of an elongated slot lip. The point where the airfoil is first cut away to form the slot on the lower surface is called the slot entry. Slot entries are often made with very small radii of curvature or provided with skirts to fair over the gap in the lower surface when the flap is retracted. By minimizing the gap, the lower surface is made as smooth as possible so that there is little increase in drag over that of the smooth airfoil.

Since a slotted flap increases the maximum lift by a combination of increased camber, increased chord, and boundary-layer control provided by flow through the slot, the important design parameters are flap deflection, flap size, the chordwise position of the slot lip, and the efficiency of the flow through the slot in providing boundary-layer control. The boundary-layer control action of the flow through the slot depends on the shape of the passage through which the air must flow. The shape of this passage is made up of a combination of slot-entry shape, slot-lip shape, flap-nose shape, and the position of the flap with respect to the slot lip. Airfoil shape can be expected to have a greater effect on the characteristics of slotted flaps than on those of plain or split flaps because of the fact that the airfoil shape determines to some extent the shape of the flap and slot configurations. Changes in Reynolds number can also have different effects on the characteristics of slotted flaps from those on the characteristics of plain or split flaps because of the scale effect on the flow through the slot.

Maximum lift.—Because of the large number of unrelated combinations of airfoils and slotted flaps for which data are available, a summary of maximum lift coefficients that have been obtained from various combinations is given in table I. Flap size, slot-lip extension, the deflection and position of the flap with respect to the slot lip, Reynolds number at which the tests were run, and rough classifications of slot-entry shape and flap-nose shape are tabulated along with notations as to whether the flap was located at its best maximum

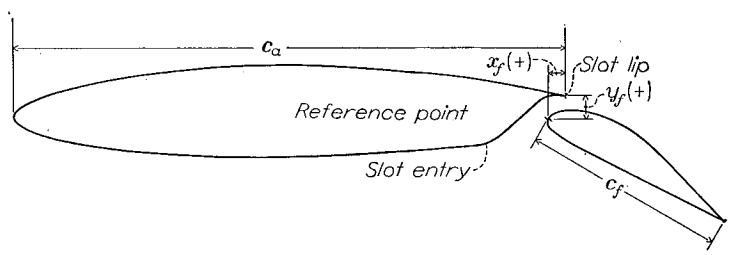

FIGURE 24.—Sketch of typical single-slotted-flap configuration. (All dimensions are given in fractions of airfoil chord.)

TABLE I.—MAXIMUM LIFT COEFFICIENTS OF AIRFOIL SECTIONS EQUIPPED WITH SINGLE SLOTTED FLAPS

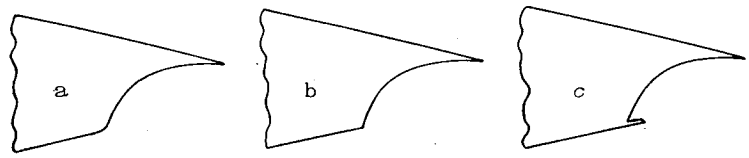

Slot-entry configurations

Flap nose shapes

Airfoil section	c_f/c	c_a	Slot-entry configuration	Flap nose shape	$c_{l_{max}}$	δ_f (deg)	x_f	y_f	Optimum position	R	Reference
Clark Y	0.20	1.00	b	A	2.44	30	0	−0.025	Yes	0.61×10	19
Clark Y	.30	1.00	b	A	2.83	40	0	−.025	Yes	.61	19
Clark Y	.40	1.00	b	A	3.10	40	0	−.025	Yes	.61	19
23012	.10	.93	a	A	2.25	50	.004	.005	Yes	3.5	11
23012	.15	1.00	b	A	2.68	30	0	.015	Yes	3.5	20
23012	.25	1.00	b	A	3.22	40	0	.015	Yes	3.5	20
23012	.256	.800	a	B	2.76	50	.005	.018	Yes	3.5	12
23012	.257	.83	a	A	2.81	50	.005	.016	Yes	3.5	12
23012	.257	.83	a	A	2.83	40	.013	.024	Yes	3.5	11
23012	.267	1.00	b	A	2.90	30	0	.025	No	3.5	12
23012	.30	.90	c	A	2.92	50	.002	.010	No	3.5	21
23012	.30	.90	c	A	2.92	40	.002	.020	No	3.5	21
23012	.30	.90	c	A	2.93	30	.002	.030	No	3.5	21
23012	.30	.90	b	A	2.88	40	.002	.020	No	3.5	21
23012	.30	1.00	b	A	3.29	40	0	.015	No	3.5	21
23012	.40	.715	b	A	2.87	50	.015	.015	Yes	3.5	22
23012	.40	.715	a	A	2.90	50	.015	.015	Yes	3.5	22
23021	.15	1.00	b	A	2.59	60	0	.015	No	3.5	23
23021	.15	1.00	b	A	2.66	60	.050	.030	Yes	3.5	24
23021	.25	1.00	b	A	3.17	40	.025	.015	Yes	3.5	24
23021	.257	.827	b	B	2.69	60	0	.015	Yes	3.5	25
23021	.257	.827	a	B	2.74	60	0	.015	Yes	3.5	25
23021	.257	.827	b	A	2.71	60	.005	.020	Yes	3.5	25
23021	.257	.827	a	A	2.82	50	0	.025	Yes	3.5	25
23021	.40	.715	b	A	2.79	50	.015	.025	Yes	3.5	26
23021	.40	.715	a	A	2.88	50	.015	.045	Yes	3.5	26
23030	.257	.860	b	B	2.59	60	.025	.040	Yes	3.5	27
23030	.257	.860	a	B	2.68	60	−.005	.040	Yes	3.5	27
23030	.40	.775	b	B	2.82	50	.025	.060	Yes	3.5	27
23030	.40	.775	a	B	2.90	50	.025	.060	Yes	3.5	27
63,4-420	.25	.88	b	B	3.00	35	.018	.045	No	6.0	7
63,4-421 (approx.)	.243	.835	a	A	3.21	40	0	.027	Yes	9.0	28
65-210	.25	.84	c	A	2.47	45	.009	.010	Yes	6.0	29
65-210	.25	.90	c	A	2.48	41.3	.014	.009	Yes	6.0	29
65-210	.25	.975	c	A	2.45	35	.004	.020	Yes	6.0	29
$65_{(112)}$A111 (approx.)	.35	.839	c	A	2.69	35	−.020	.032	Yes	9.0	30
65_1-213 (approx.)	.336	.889	c	A	2.63	40	.019	.046	No	9.0	31
$65_{(215)}$-114	.259	.915	c	A	2.80	40	.019	.038	No	9.0	31
65,2-221 (approx.)	.263	.832	a	B	2.83	30	.025	.046	Yes	9.95	32
66(215)-116, a=0.6	.25	.824	c	B	2.70	55	0	.028	No	6.0	33
66,2-116, a=0.6	.25	.827	a	A	2.69	45	.017	.038	No	6.0	34
66,2-216, a=0.6	.30	.90	c	A	2.92	37	0	.016	No	6.0	7
66,2-216, a=0.6	.25	.824	a	A	2.89	40	.023	.040	Yes	5.1	35
66,2-216, a=0.6	.25	.834	c	A	2.88	45	.011	.031	Yes	5.1	35
66,2-118	.25	.90			2.68	32.5	--------	--------	No	6.0	36
Davis $\frac{t}{c}$=0.18	.30	1.00	b	A	3.45	40	--------	--------	No	6.2	37
Davis (modified) $\frac{t'}{c}$=0.18	.30	1.00	b	A	3.14	40	--------	--------	No	6.0	37
66-series (approx.) $\frac{t}{c}$=0.18	.30	1.00	b	A	3.34	30	--------	--------	No	6.2	37

lift position. References from which the data were obtained are also given in the table (references 11, 12, and 19 to 37). Maximum lift coefficients of airfoils with slotted flaps are shown to be considerably higher than those of the same airfoils equipped with plain or split flaps of comparable size. The advantage of the higher maximum lift coefficients must be balanced, however, against the added complication of providing external brackets to hold the flap or of more complicated mechanisms required to operate the flap.

Maximum lift coefficients are shown in figure 25 plotted against flap deflection for the NACA 23012 airfoil section with various sizes of slotted flaps and in figure 26 for two NACA 6-series airfoils with slotted flaps. These data and the data of table I show that the flap deflections for maximum lift coefficients of airfoils with slotted flaps vary over a range of from about 30° to over 60°. Although no rigid variation of optimum deflection with flap size or slot-lip extension can be shown, it may be seen from the data in table I that flaps with the slot lip extended to the trailing edge seem to show their highest maximum lift coefficients at lower flap deflections than with shorter slot-lip extensions.

The effect on maximum lift coefficient of increasing the effective chord of the airfoil-flap combination is shown in figure 27 for various flap combinations on the NACA 23012 airfoil section. The maximum lift coefficients are all based on the chord of the airfoil with flap completely retracted. Maximum lift coefficients are shown to increase as the total chord is increased either by increasing the flap chord or the slot-lip extension. Increases in flap size above about 25 percent of the airfoil chord are shown to have much smaller effects on maximum lift coefficients than increases in the lower range of flap size. Increases in slot-lip extension, however, seem to be more effective as the slot lip is extended toward the trailing edge. Although the variations of maximum lift coefficient shown in figure 27 cannot be expected to hold strictly for different types of airfoil section, the

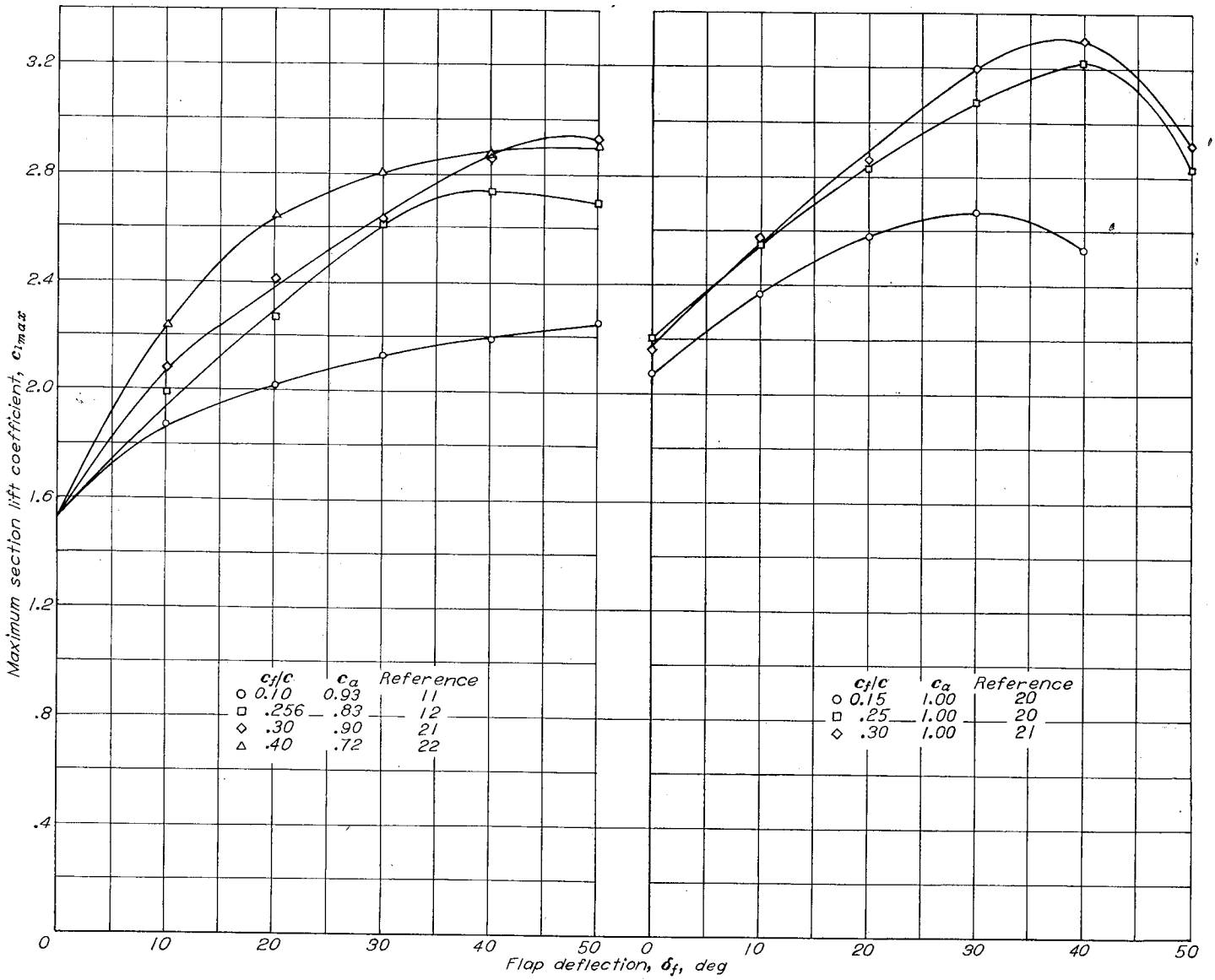

FIGURE 25.—Variation of maximum section lift coefficient with flap deflection for the NACA 23012 airfoil equipped with various slotted flaps. $R=3.5\times10^6$.

variations shown are probably indicative of the results to be expected from conventional airfoils of normal thicknesses. The use of thinner airfoils, however, and particularly thin NACA 6-series sections, presents added difficulties because of the very thin flaps and very small leading-edge radii of the flaps that can be fitted into the available space. The data shown in table I for 25-percent-chord flaps on the NACA 65–210 airfoil section with various slot-lip extensions show that no increase in maximum lift coefficient is obtained by increasing the slot-lip extension from 84 percent chord to 97.5 percent chord.

The most favorable shape for the passage through which the air must flow from the lower surface over the flap is an extremely complex problem since it involves a combination of several variables, each of which can have a large effect on the flow condition produced by each of the other variables. These variables include flap shape, slot-entry shape, slot-lip shape, and flap position.

Data are given in references 12, 25, and 28 on the maximum lift coefficients produced by slotted flaps of various shapes. No strict rules can be set down for the design of flap shapes, but from the data given in these references, it is generally observed that a flap-nose shape similar to the shape of a good airfoil will provide good maximum lift characteristics.

Slot-entry shapes can have a large effect on maximum lift coefficients since any separation of the flow at the slot entry can block off a portion of the slot passage. Data are available in references 12, 21, 22, 25 to 28, 32, 34, and 35 which show the effects of various slot-entry shapes on maximum lift coefficients. Data in references 22, 25 to 27, and 35 show maximum lift coefficients that have been obtained on NACA 23012, 66,2–216, 23021, and 23030 airfoil sections equipped with slotted flaps and with both smoothly rounded and sharp slot entries. In these references, the best position of the flap was determined with each of the slot entries. Neither the 0.12c-thick nor the 0.16c-thick airfoils showed any difference in best maximum lift coefficient although the position of the flap at which the best maximum lift coefficient was measured changed considerably. Both the 0.21c-thick and the 0.30c-thick airfoils on the other hand showed large effects of slot-entry configuration. These data would seem to indicate that the airfoil thickness or the depth of the flap well (opening into which flap retracts) would determine whether the slot entry has an effect on the maximum lift coefficient.

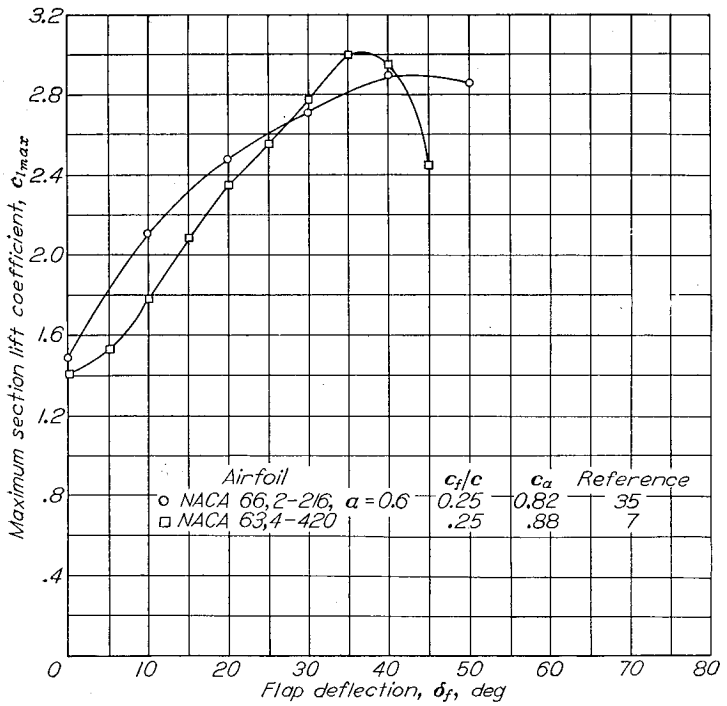

FIGURE 26.—Variation of maximum section lift coefficient with flap deflection for several NACA 6-series airfoil sections equipped with slotted flaps. $R=5.1\times10^6$ for NACA 66-series airfoil and $R=6.0\times10^6$ for NACA 63-series airfoil.

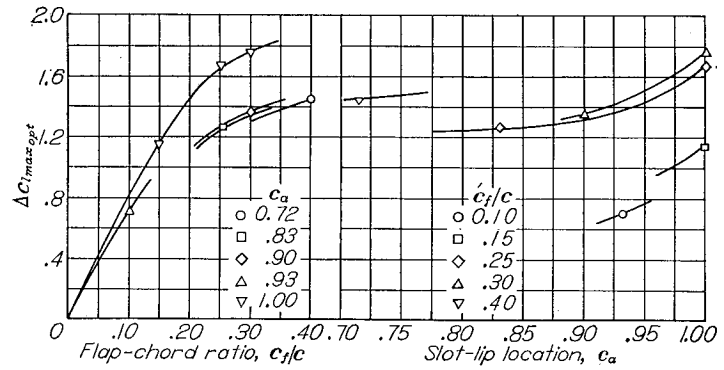

FIGURE 27.—Variation of optimum increment of section maximum lift coefficient with flap-chord ratio and with slot-lip location for the NACA 23012 airfoil section.

For the thick airfoils where the slot-entry configuration can have an effect, the smoothly rounded entry provides the highest maximum lift coefficient in each case. Data from reference 34 are shown in figure 28 for an NACA 66,2-116, $a=0.6$ airfoil equipped with a $0.25c$ slotted flap with three different lengths of slot-entry skirt. These data show that with the flap located at an arbitrary position, the maximum lift coefficient was lowered by each progressive extension of the slot-entry skirt.

Slot-lip shape can affect the maximum lift coefficients of airfoil-flap combinations to a large extent and it is felt that the most important requirement of a good slot-lip shape is that it should serve to direct the air flow downward over the flap. Data are shown in figure 29 for an airfoil with a slotted flap with the slot lip in its normal configuration and bent down various amounts. These data show that the maximum lift coefficient is increased by bending down the slot lip, although too great a bend causes the maximum lift coefficient to drop off. It is believed that the limit in the effect of bending down the lip is reached when the flow over the lip itself separates.

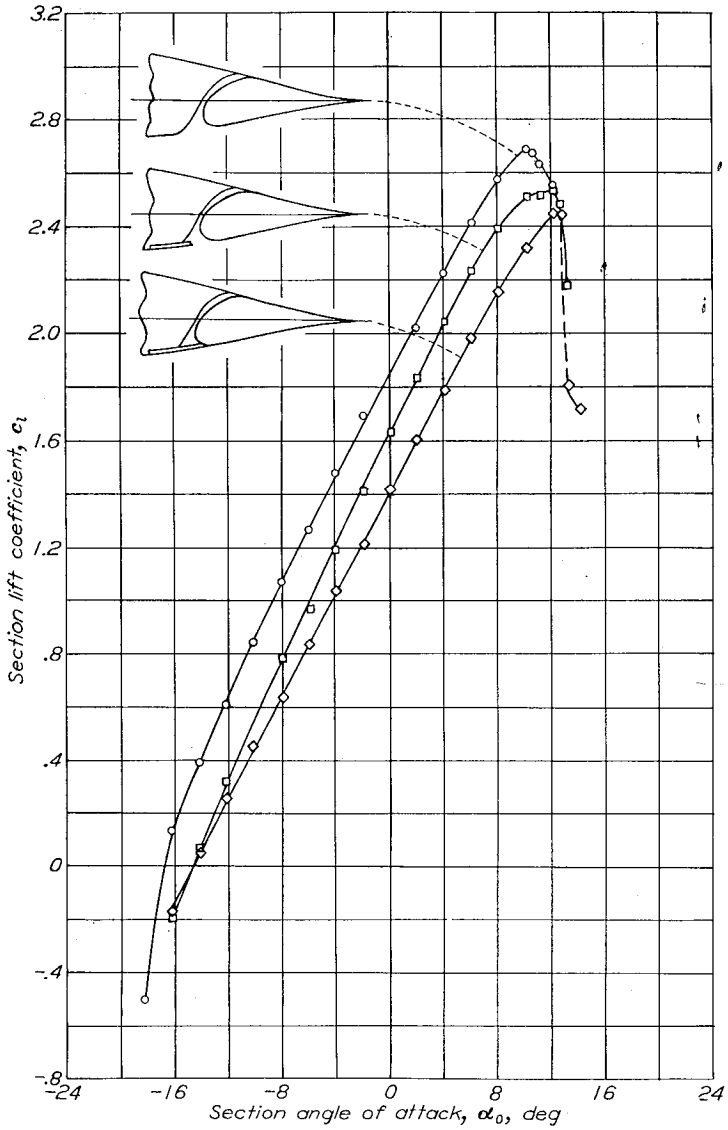

FIGURE 28.—Effect of slot-entry-skirt extension on section lift characteristics of an NACA 66, 2-116, $a=0.6$ airfoil equipped with a $0.25c$ slotted flap deflected 45°. $R=6.0\times10^6$; reference 34.

The flap location affects the maximum lift coefficient, of course, by changing both the shape and size of the passage through which the air flows from the lower surface. The best flap position will, therefore, be different for each different condition of slot entry, slot lip, and flap-nose shape. No general conclusions can be drawn concerning the best location of a slotted flap although the data available in references 12, 19, 20, 22, 24 to 27, 29, 30, and 32 to 35 should be useful for the design of the best flap location for airfoil-flap combinations similar to those for which data are available. Generally, it may be said that the best location of a flap of a given shape will be a location which, when combined with the slot lip and slot entry, will provide a converging passage and allow the flow to be directed downward over the flap. Data in figure 30, for instance, show lift characteristics of an airfoil-flap combination for which the slot does not form a converging passage. A comparison of these data with those in table I for airfoils of similar thickness shows the low maximum lift coefficients obtained with a flap configuration of this type. Contours of flap position for maximum lift coefficient are shown in figure 31 for two airfoil sections

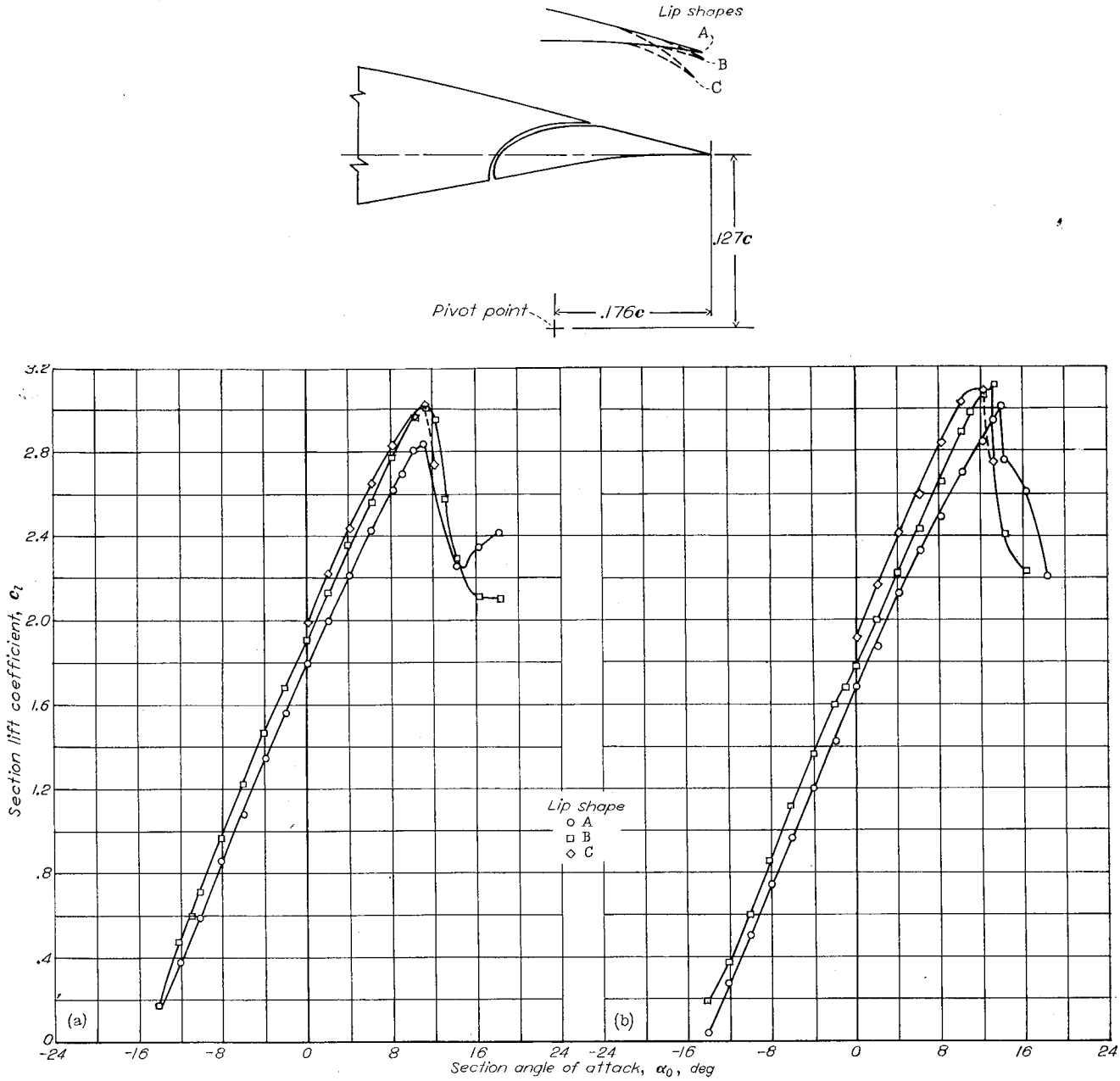

(a) Flap deflection, 35°. (b) Flap deflection, 40°.

FIGURE 29.—Effect of slot-lip shape on section lift characteristics of an NACA 63,4-420 airfoil equipped with a 0.25c slotted flap. R=6.0×10^6.

equipped with various configurations of slotted flaps. These contours indicate the sensitivity of the maximum lift coefficient to small changes in flap position and the accuracy with which the flap must be built and located.

Airfoil shape can have a large effect on the effectiveness of slotted flaps. There are not, however, enough data for flaps of similar size and shape to show fully the effects of the various airfoil design parameters on the maximum lift coefficients of airfoils with slotted flaps. Some data are shown in figure 32 for NACA 230-series airfoils of various thicknesses with flaps of two different sizes and a few data for various NACA 6-series sections with 0.25c slotted flaps. Although not at all conclusive, these data for NACA 6-series airfoils seem to show a greater effect of thickness ratio than was previously indicated (reference 27) by the NACA 230-series data. While a part of the differences between the 230-series sections and the 6-series sections might be attributed to the higher Reynolds number at which the latter data were obtained, data in reference 28 on the 0.21c-thick 6-series airfoil show that even at a Reynolds number of 2.0×10^6 the maximum lift coefficient of this airfoil is above 3.0.

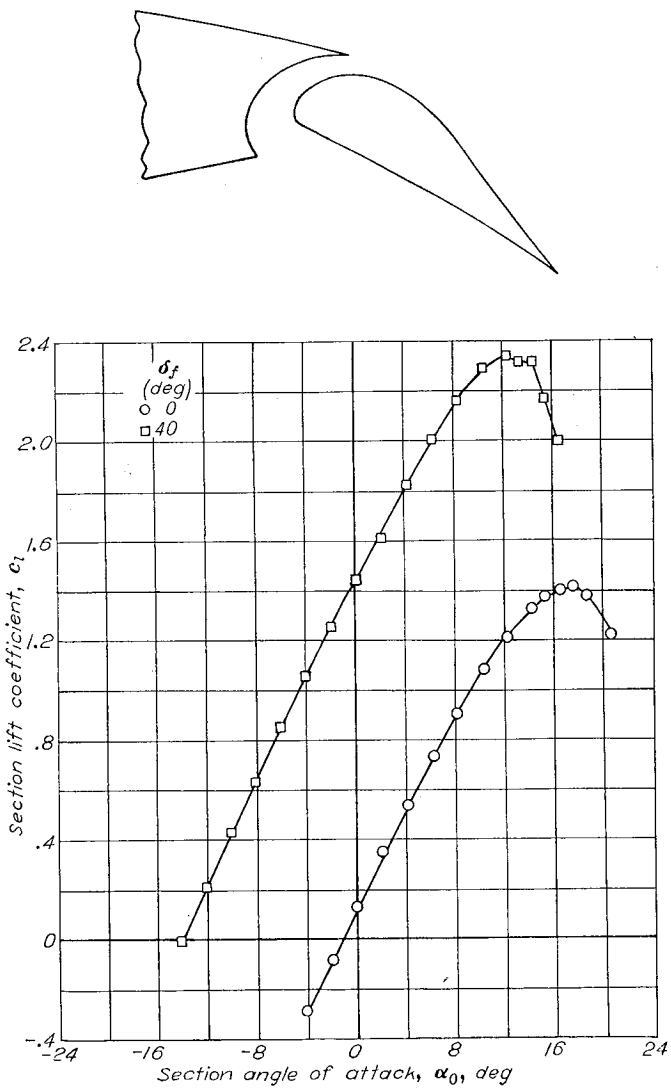

FIGURE 30.—Lift characteristics of an approximate NACA 66(215)-216 airfoil section equipped with a 0.25c slotted flap. R=6.0×10⁶.

Data on the effect of Reynolds number on the maximum lift coefficients attainable with slotted flaps are given in references 12, 25, 27 to 33, and 37. The greater part of these data covers Reynolds numbers from about 3.0×10^6 to 10.0×10^6. A few data are given, however, for higher Reynolds number. Maximum lift coefficients are shown plotted against Reynolds number in figure 33 for two NACA 6-series airfoils with slotted flaps. In both of these cases, the scale effect with flap deflected is approximately the same as that for the plain airfoil. This similarity cannot be considered to be true in the general case, however. There are some indications that the best maximum-lift position of a slotted flap may change with changes in Reynolds number as shown in reference 30. From these data it is seen that for the changes in Reynolds number shown (from 2.4×10^6 to 9.0×10^6) an appreciable change in best position for maximum lift is noted and that for this airfoil-flap combination, at least, the best position moves backward and upward as the Reynolds number is increased. The maximum lift coefficient at a Reynolds number of 9.0×10^6 was increased by about 0.06 by changing from the position found to be best at $R=2.4\times10^6$ to the position at which the highest maximum lift coefficient was measured. In this case, the entire character of the lift curve was changed by this change in positions at $R=9.0\times10^6$ although this change cannot be considered typical.

Data on the effects of roughness on the maximum lift coefficients of airfoils with slotted flaps are not extensive enough to provide any generalizations although it may be said that the decrement in maximum lift coefficient caused by roughness will be of about the same order of magnitude as for airfoils with split flaps. It must be remembered therefore that leading-edge roughness can cause the maximum lift coefficient of airfoils to be 0.4 to 0.5 lower than that obtained in a wind tunnel with a smoothly polished model. Some data are shown in references 29 to 31 on the effects of roughness on the maximum lift coefficient of airfoils with slotted flaps.

Drag.—Drag coefficients of airfoils equipped with slotted flaps can be expected to be lower than those of airfoils with either plain or split flaps because of the fact that the separation of the flow over the flap, usually apparent on plain flaps at high deflections, and the wide, blunt rear portion of airfoils equipped with split flaps are eliminated or minimized with slotted flaps. Envelope polars for the NACA 23012 airfoil equipped with slotted flaps of various sizes are shown in figure 34. These data show an effect of increasing flap size that is opposite to that with either plain or split flaps, the drag decreasing at a given lift coefficient as the flap size is increased. The drag polar for the NACA 23012 airfoil equipped with a 0.40c split flap is also shown in figure 34 and indicates the much lower drag coefficients obtained with slotted flaps than with split flaps. The effect of slot-lip extension on drag is shown in figure 35. Increasing the slot-lip extension also is shown to decrease the drag at any given lift coefficient.

Flap position can also have a great effect on drag coefficients since the shape of the slot passage determines whether there are any areas of separated flow in the region of the flap. Contours of flap position for minimum drag coefficient are shown for various airfoil-flap combinations in references 20, 22, 24, 26, 27, and 35. One of these contours taken from reference 35 is shown in figure 36. These data and those given in the references show that the requirements of a good slot shape for low drags are different from the requirements for high maximum lift coefficients. The slots for which low drags are measured seem to be nearly constant in area rather than converging, and the slot openings seem to be larger than those for high maximum lift.

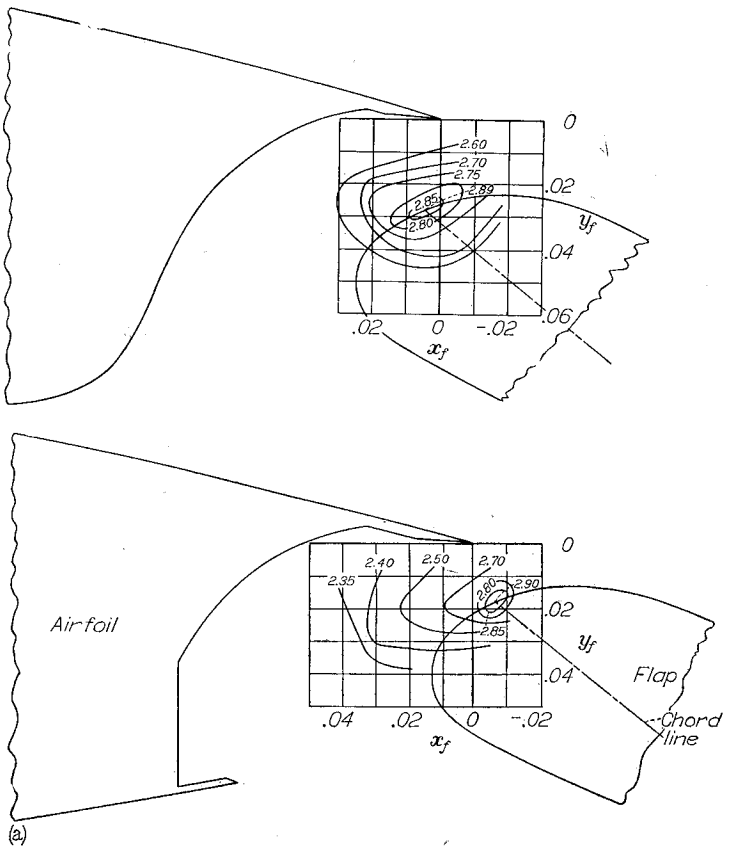

(a) NACA 66, 2-216, a=0.6 airfoil with 0.25c slotted flap and two slot-entry configurations. R=5.1×10⁶; δ_f=40°; reference 35.

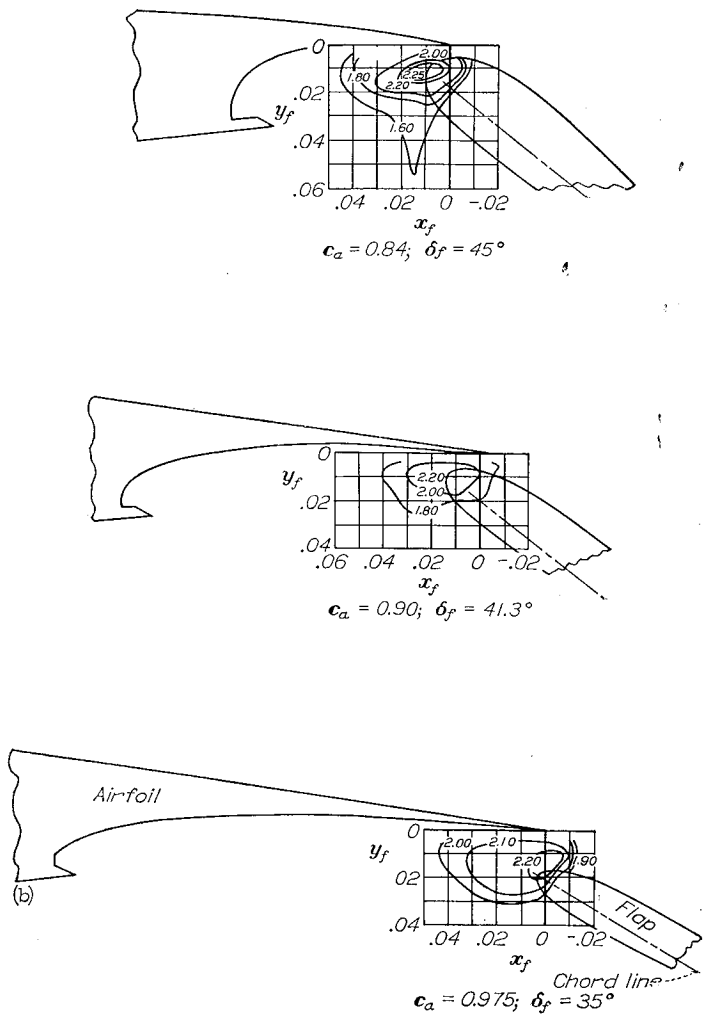

(b) NACA 65-210 airfoil with 0.25c slotted flap and three slot-lip locations. R=2.4×10⁶; reference 29.

FIGURE 31.—Contours of flap position for maximum section lift coefficient for two airfoils equipped with slotted flaps.

FIGURE 31.—Concluded.

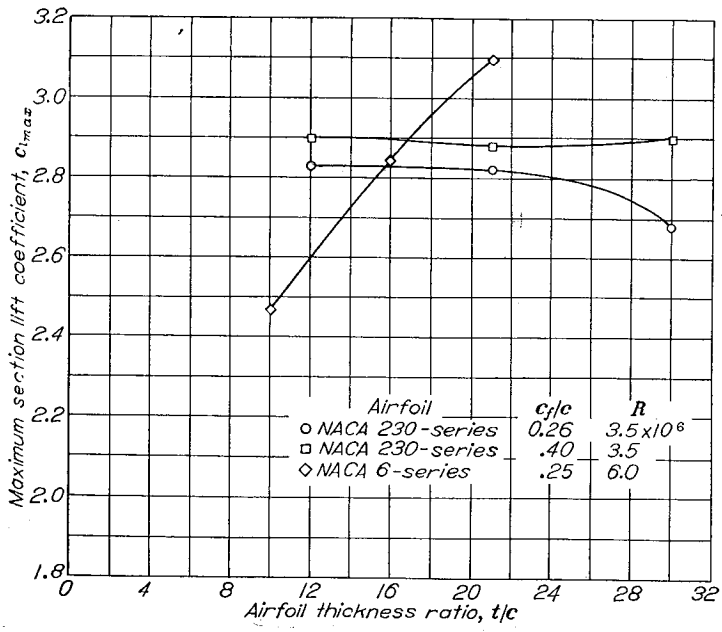

FIGURE 32.—Effect of airfoil thickness ratio on section maximum lift coefficients of airfoils equipped with single slotted flaps.

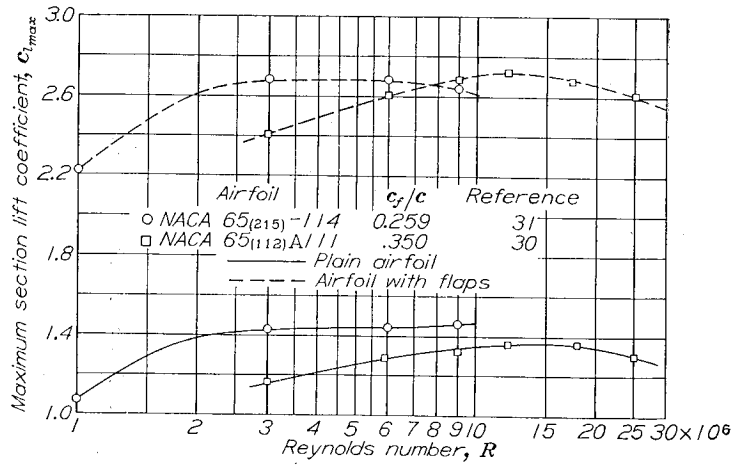

FIGURE 33.—Scale effect on maximum section lift coefficient for two low-drag airfoil section equipped with slotted flaps.

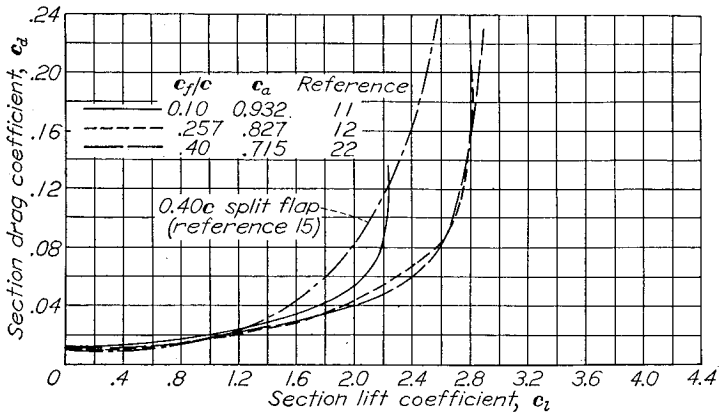

FIGURE 34.—Effect of flap size on envelope drag polars for an NACA 23012 airfoil equipped with single slotted flaps. $R=3.5\times10^6$.

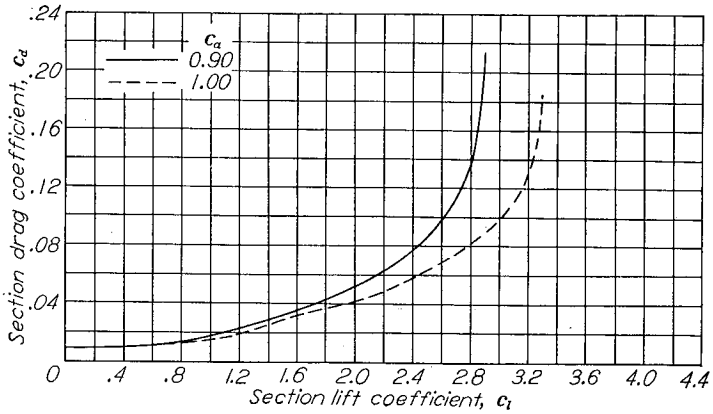

FIGURE 35.—Effect of slot-lip extension on envelope drag polars. NACA 23012 airfoil, $\frac{c_f}{c}=0.30$; $R=3.5\times10^6$. Reference 21.

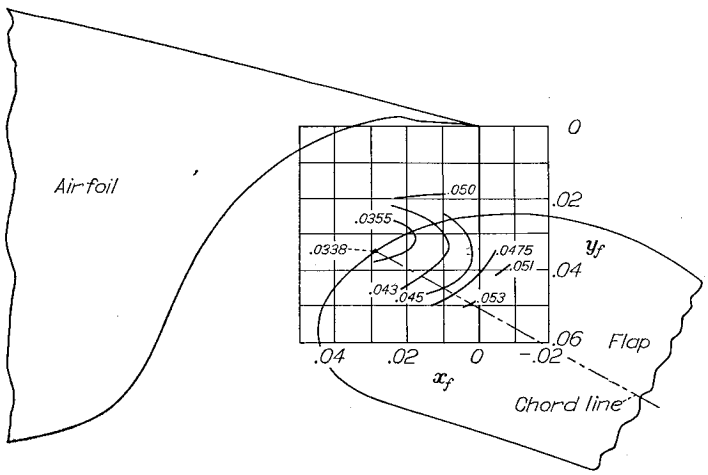

FIGURE 36.—Contours of flap position for various section drag coefficients for the NACA 66,2-216, $a=0.6$ airfoil equipped with a 0.25c slotted flap. $\delta_f=30°$; $c_l=2.5$; $R=5.1\times10^6$; reference 35.

With slotted flaps in the retracted position, the resulting break in the airfoil lower surface has been shown to have large effects on drag coefficients. Drag data are shown in figure 37 for an NACA 6-series airfoil section equipped with a 0.25c slotted flap. These data show that when air is allowed to leak through the gap, the drag increment in the low-drag range caused by a sharp slot entry is approximately twice that caused by a well-rounded entry. These data also show, however, that the drag coefficient with the sharp entry can be reduced to the same value as with the rounded slot entry merely by sealing the gap to prevent any flow of air. Data are shown in figure 38 for an NACA 66,2–116, $a=0.6$ airfoil with a 0.25c slotted flap and three lengths of slot-entry-skirt extension. These data show that the drag is progressively lowered as the slot-entry skirt is extended.

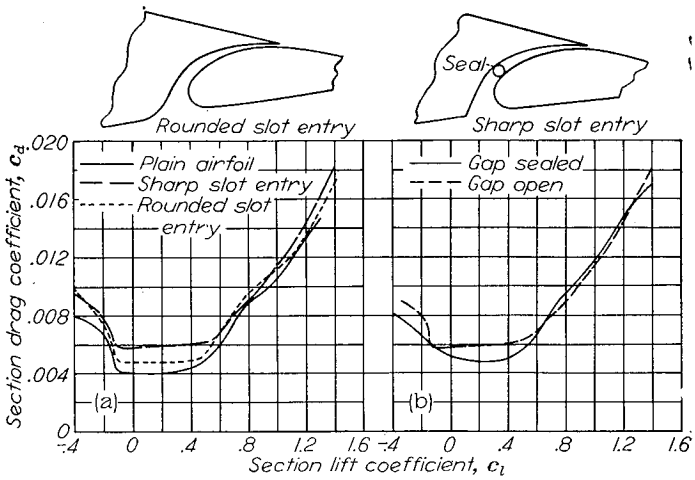

(a) Gap open. (b) Sharp slot entry.

FIGURE 37.—Effect of slot opening and gap seal on drag coefficient of an NACA 65(216)-3(16.5) (approx.) airfoil equipped with a 0.25c slotted flap. $R=6.0\times10^6$.

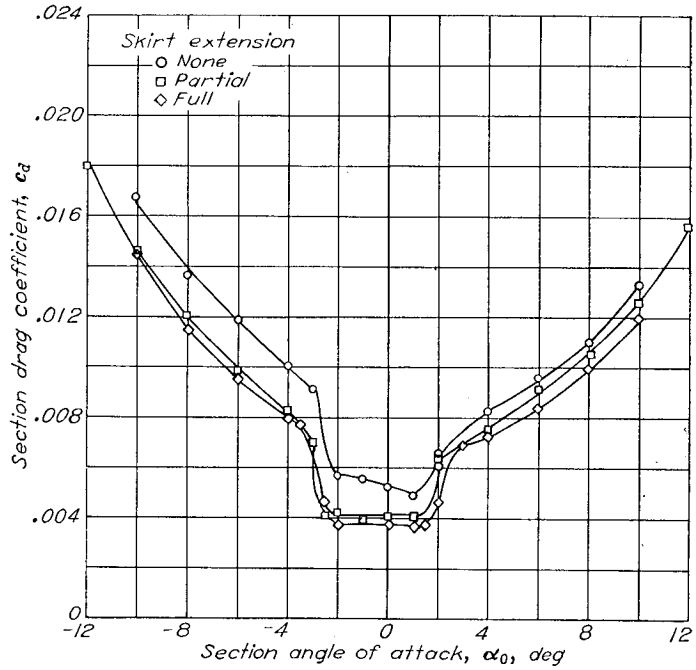

FIGURE 38.—Effect of slot-entry-skirt extension on section drag characteristics of an NACA 66,2-116, $a=0.6$ airfoil equipped with a 0.25c slotted flap. $\delta_f=0°$; $R=6.0\times10^6$; reference 34. (Same airfoil-flap combination as fig. 28.)

Pitching moment.—Since a slotted flap is similar to a plain flap with a boundary-layer-control slot at the flap nose, the load distribution over an airfoil with a slotted flap should be similar to that over an airfoil with a plain flap with the exception of discontinuities at the slot. The pitching moments of airfoils equipped with slotted flaps should be approximately the same as the pitching moments of an airfoil with a plain flap of similar size. The flap-chord ratio and the airfoil chord must be defined for this purpose, however, on the basis of the total chord with flap extended. Pitching-moment slopes have been calculated on the basis of total chord with flap extended for several combinations of airfoil and slotted flaps and are shown in figure 39 along with the slopes calculated from the thin-airfoil theory. These data show that the pitching moments of airfoils with slotted flaps approximate those predicted by the plain-flap theory although the experimental pitching moments for slotted flaps are in all cases slightly higher than the theory indicates and show considerably less variation with flap size than the theoretical.

Flap loads and moments.—Aerodynamic load characteristics for a number of airfoils equipped with slotted flaps are presented in references 19, 33, 38, and 39. Flap loads generally increase as the flap deflection is increased up to the deflection at which the flap stalls, the variation in flap loads with angle of attack for unstalled conditions being small as compared with the variation with flap deflection. Normal-force coefficients on slotted flaps for the data shown in the references usually reach a maximum of about 1.6 or 1.8. Chord forces are generally small compared with the normal forces, and centers of pressure of the flap loads usually range from about 0.2 to 0.4 of the flap chord.

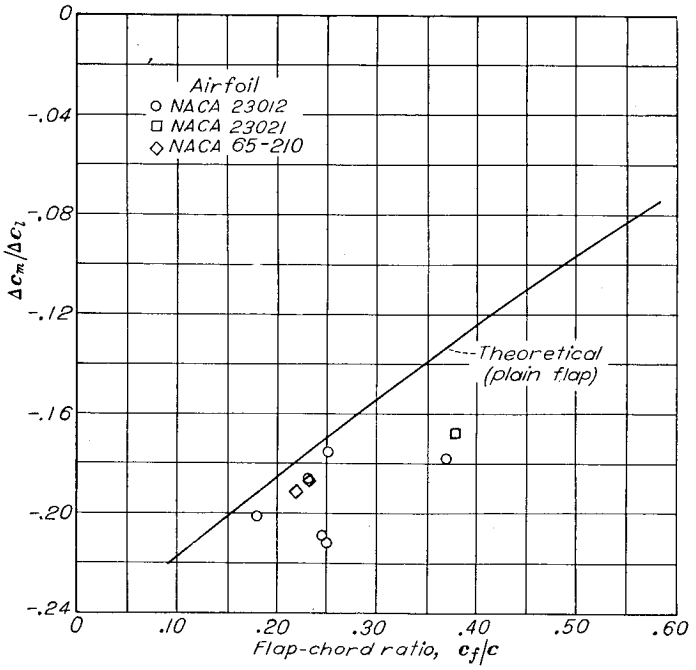

FIGURE 39.—Variation of ratio of increment of section pitching-moment coefficient to increment of section lift coefficient with flap-chord ratio for several airfoil sections with slotted flaps. $\alpha_0=0°$. (All coefficients based on total chord with flap extended.)

DOUBLE SLOTTED FLAPS

Data are presented in reference 11 for an NACA 23012 airfoil equipped with a 0.256c slotted flap and several auxiliary flaps. These data show that the slotted flap with a 0.10c auxiliary slotted flap was more effective in increasing the maximum lift coefficient than any of the other devices tested. Reference 40 shows data for NACA 23012, 23021, and 23030 airfoils equipped with 0.40c slotted flaps and 0.256c auxiliary slotted flaps. Maximum lift coefficients of 3.46, 3.57, and 3.71, respectively, were measured with these double slotted flaps on the three airfoils. Later investigations showed that the double slotted flap could be simplified considerably by changing the form of the foreflap to a turning vane. For double slotted flaps of a given total chord, the vanes were shown to be just as effective as the foreflaps tested on the original double slotted flaps and had the added advantage of being of such a size that they could be entirely enclosed within the wing structure when the flap was retracted. A typical double slotted flap of the latter type is shown in figure 40. The slot entry and slot lip are defined in the same way as for single slotted flaps. The vane chord line has been defined in various ways, but the most frequently used definitions are the maximum-length line or the line through the trailing edge and the center of curvature of the vane leading edge. The vane size is then defined by the length of this chord line and the deflection, by the angle between the airfoil chord line and the vane chord line.

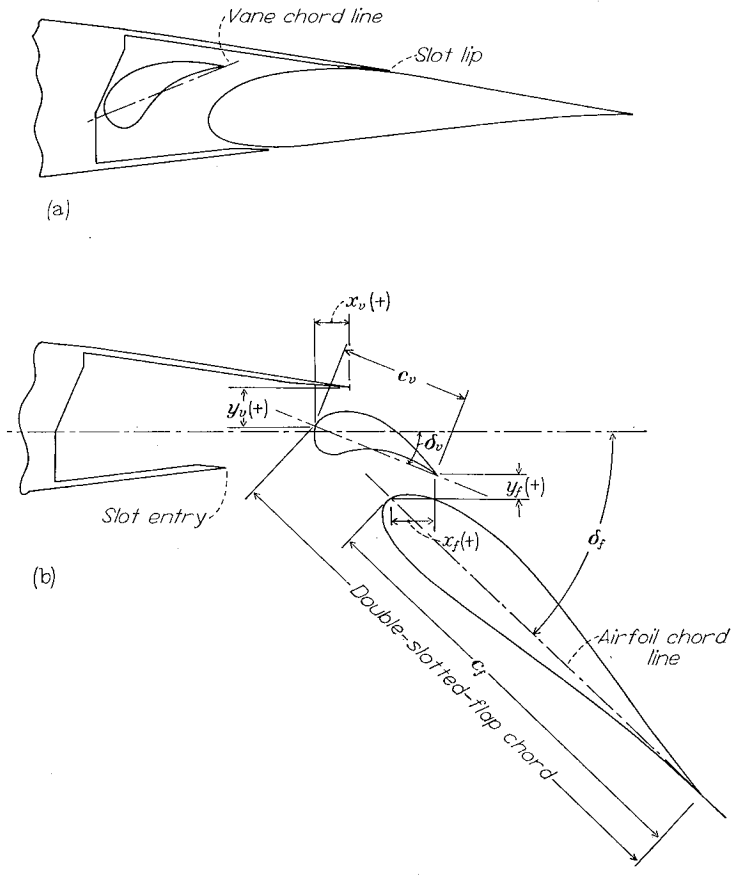

(a) Flap retracted.
(b) Flap deflected.

FIGURE 40.—Sketch of typical double-slotted-flap configuration. (All dimensions are given in fractions of airfoil chord.)

Double slotted flaps operate to increase the maximum lift coefficient in essentially the same way as single slotted flaps with the exception that an additional slot is available to provide a greater amount of boundary-layer control. Another way of defining the action of a double slotted flap is that it is merely a single slotted flap which is provided with a turning vane in the slot to help deflect the air flow downward over the flap, since the downward deflection of the flow is the principal function of the vane. As a result of its turning action, however, the vane also carries an appreciable lift load of itself. The important design parameters are, as is the case for single slotted flaps, flap deflection, flap size and extension, and the efficiency of the flow through the slot passages in preventing separation.

Maximum lift.—Maximum-lift data for airfoils with double slotted flaps are presented in table II along with information concerning the flap and airfoil configuration and test conditions, as well as the references from which the data were obtained (references 11 and 40 to 51). Although the absolute optimum positions of both flap and vane were not determined for all the configurations which are noted as optimum positions in the table, this notation does indicate that enough tests were made to determine a position at which the maximum lift coefficient is essentially the optimum. Double slotted flaps are seen to produce higher maximum lift coefficients than any of the other flaps so far considered.

Flap deflections at which the highest maximum lift coefficients were measured as shown in table II varied from 45° to 70° and vane deflections varied from 20° to 30°. Although the data are rather scattered, a general trend toward higher flap deflections and lower vane deflections can be noted as the airfoil thickness ratio is increased.

Although a fairly large amount of data is available, the effects of flap size and extension are not well defined because of the fact that most of the designs tested up to the present time are of approximately the same size. The data in references 11 and 40 on NACA 230-series airfoils equipped with the original type of double slotted flap give an indication, however, that larger double slotted flaps (up to 0.40c, at least) should provide higher maximum lift coefficients than those obtained with flaps of the sizes normally employed. Some few data are available in references 41 to 43 on the effect of vane size on the maximum lift coefficients obtainable for several airfoil sections equipped with double slotted flaps. Some of these data are presented in figure 41 and show that, in general, increases in vane size provide increases in maximum lift coefficients although the range of vane size covered is rather small.

The available data on the effects of slot-entry and slot-lip configurations are also meager. The effects of the shape of the slot can be expected, however, to be similar to those noted for single slotted flaps. The effects of slot-entry-skirt extension on the lift characteristics of an airfoil section equipped with a double slotted flap operating along a fixed flap path are presented in figure 42. Although the lift coefficients at the highest flap deflections were not affected by the extension of the slot-entry skirt, those at intermediate deflections were lowered considerably by the longest extension.

Some data on the effect of flap and vane positions on maximum lift coefficients are given in references 41 to 43, 46, 49, and 50. From the data for optimum configurations shown in table II it may be seen that vane positions for best maximum lift coefficients usually fall within a range of position from 0.018c to 0.025c below the slot lip and from 0.005c to 0.015c forward of the slot lip although a few of the data show that highest maximum lift coefficients were measured with the vane located about 0.005c behind the slot lip. The positions of the flap cover a wider range varying from 0.015c to 0.030c forward and from 0.005c to 0.020c below the vane trailing edge. In one case, the flap was found to give the highest maximum lift coefficient when located behind the vane trailing edge. Although the data in table II show that flap and vane positions for maximum lift fall within a fairly well-defined range of positions, care should be exercised in setting flap and vane positions arbitrarily from these data because of the great sensitivity of these flaps to small changes in position. A few contours of flap and vane positions for maximum lift coefficient are shown in figure 43 and indicate the accuracy with which the flap and vane must be located.

TABLE II.—MAXIMUM LIFT COEFFICIENTS OF AIRFOIL SECTIONS EQUIPPED WITH DOUBLE SLOTTED FLAPS

Airfoil section	c_f/c	c_v/c	c_a	$c_{l_{max}}$	δ_f (deg)	δ_v (deg)	x_f	y_f	x_v	y_v	Optimum position	R	Reference
23012	0.10	0.189	0.83	2.99	70	40	0.009	0.009	0.014	0.024	Yes	3.5×10^6	11
23012	.257	.227	.715	3.47	70	30	.014	.012	.015	.035	No	3.5	40
23021	.257	.227	.715	3.56	60	30	.019	.024	.025	.065	No	3.5	40
23030	.257	.260	.715	3.71	80	40	.049	.050	.045	.040	No	3.5	40
23012	.257	.117	.826	3.30	60	25	−.016	.010	−.004	.017	Yes	3.5	41
23021	.257	.147	.827	3.32	70	30	.017	.027	.007	.024	Yes	3.5	42
63–210	.25	.075	.84	2.91	50	25	.022	.024	.024	.013	Yes	6.0	43
63,4–421 (approx.)	.195	.083	.87	3.30	55	14	.038	.012	−.009	.016	No	6.0	(a)
64–208	.25	.075	.84	2.51	45	30	.015	.015	.015	.019	Yes	6.0	43
64–208	.25	.056	.84	2.40	50	25	.018	.014	.015	.024	Yes	6.0	43
64–210	.25	.075	.84	2.82	55	30	.023	.006	.012	.018	Yes	6.0	43
64_1–212	.25	.075	.84	3.03	50	30	.021	.020	.010	.019	Yes	6.0	43
64_1A212	.229	.083	.833	2.83	55	26	.044	.005	.004	.014	Yes	6.0	44
65–210	.25	.075	.84	2.72	50	25	.025	.011	.009	.024	Yes	6.0	43
65(216)–215, a=0.8	.248	.096	.82	3.38	70	12	.024	.010	.025	.032	No	6.3	45
65_3–118	.244	.10	.864	3.35	65	23	.038	.007	.009	.025	Yes	6.0	46
65_3–418	.236	.106	.851	3.50	65	21	.027	.007	.012	.028	Yes	6.0	47
65_4–421	.236	.109	.85	3.08	51	20	.029	.017	.012	.024	Yes	2.2	48
66–210	.25	.075	.84	2.64	55	25	.029	.023	.012	.022	Yes	6.0	43
66–210	.25	.100	.84	2.72	60	25	.027	.039	.024	.021	Yes	6.0	43
66_2–214 (approx.)	.227	.085	.854	3.00	55	20	.044	.009	.004	.025	Yes	9.0	49
1410	.25	.075	.84	3.06	50	25	.026	.016	.012	.019	Yes	6.0	43
Republic 6-series type $\frac{t}{c}$=0.17	.238	.092	.88	3.55	60	25	.015	.020	−.005	.020	Yes	3.5	50
Republic 6-series type $\frac{t}{c}$=0.17	.238	.092	.88	3.43	60	25	.015	.020	−.095	.020	Yes	14.0	50
Douglas 7-series type $\frac{t}{c}$=0.154	.250	.056	.82	3.15	50	19	.017	.016	.012	.024	No	6.0	51

[a] See figure 42.

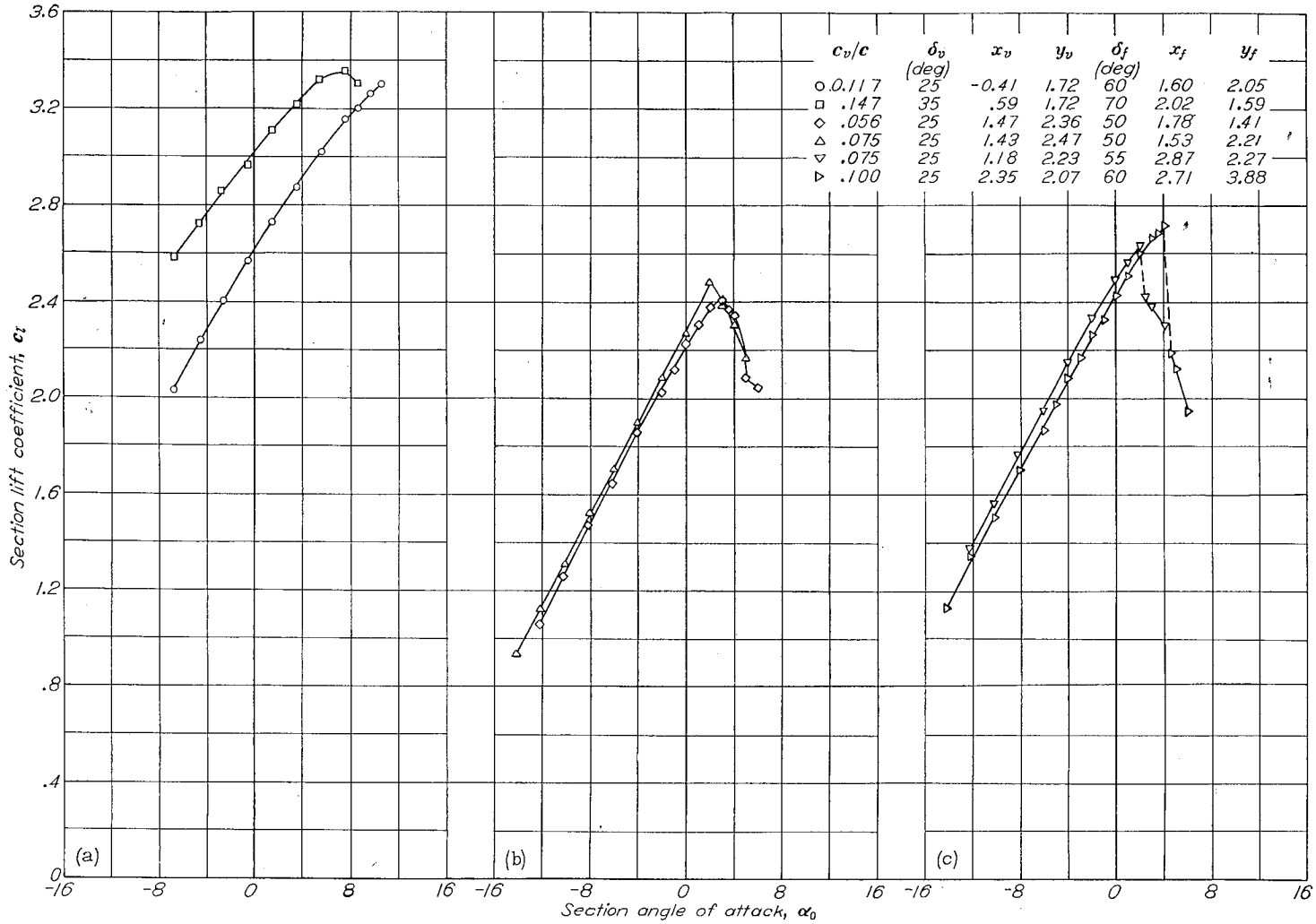

(a) NACA 23012 airfoil; $R=3.5\times10^6$; reference 41.

(b) NACA 64-208 airfoil; $R=6.0\times10^6$; reference 43.

(c) NACA 66-210 airfoil; $R=6.0\times10^6$; reference 43.

FIGURE 41.—Effect of vane size on lift characteristics of several airfoil sections with double slotted flaps.

The fact that most of the data for double slotted flaps have been obtained for configurations of roughly similar size provides a fairly extensive amount of data on the effect of airfoil section on maximum lift coefficients. Data from table II on the maximum lift coefficients of various airfoil sections with double slotted flaps are shown in figure 44 plotted against airfoil thickness ratio. All of the double slotted flaps for which data are shown had total chord lengths (from nose of vane to trailing edge of flap) of about 0.30c to 0.35c and had slot lips located at about 0.85c. Although these data are rather scattered, they define fairly well the variation of maximum lift coefficients with the various airfoil parameters. Increases in camber and forward movements of the position of minimum pressure of NACA 6-series airfoils seem to provide increases in maximum lift coefficient. Maximum lift data for NACA 63-series and 66-series sections with design lift coefficients of 0.2 equipped with 0.20c split flaps deflected 60° are also shown in this figure. These data show that the effects of thickness and position of minimum pressure can be shown qualitatively at least by the systematic split-flap data in reference 7. A comparison of the data in figures 44 and 17 shows that the effects of camber on maximum lift coefficient are approximately of the same order of magnitude for the systematic split-flap data and the double-slotted-flap data.

Scale-effect data on various airfoil-double-slotted-flap combinations are presented in references 43, 45, and 47 to 50. These data show approximately the same characteristics as the scale-effect data on single slotted flaps, and there are indications that the best maximum lift configurations of double slotted flaps may also change as the Reynolds number is changed.

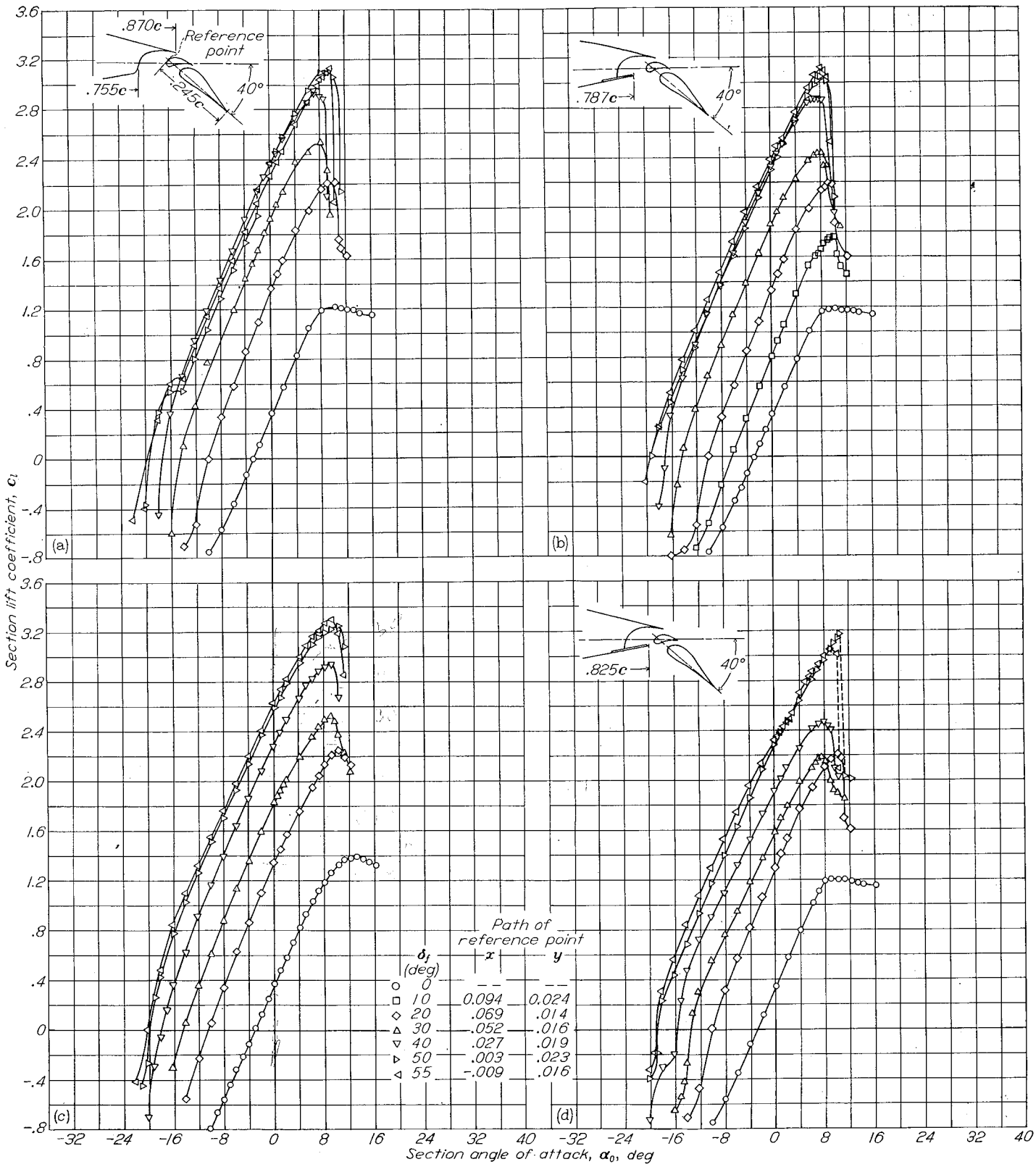

(a) No skirt extension; $R=2.4\times10^6$.

(b) Partial skirt extension: $R=2.4\times10^6$.

(c) Partial skirt extension; $R=6.0\times10^6$.

(d) Full skirt extension; $R=2.4\times10^6$.

FIGURE 42.—Section lift characteristics of an NACA 63,4-421 (approx.) airfoil equipped with a double slotted flap and several slot-entry-skirt extensions.

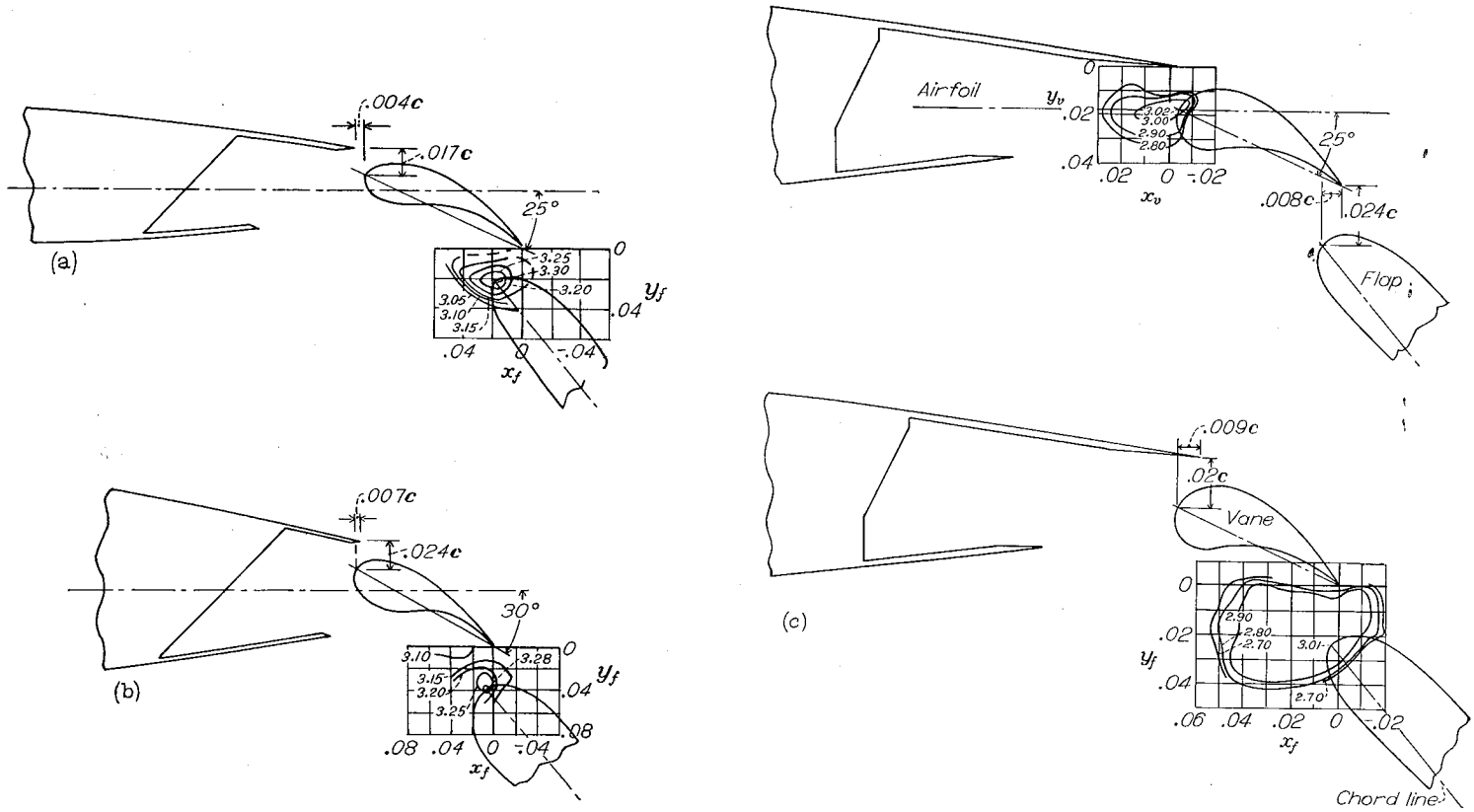

(a) NACA 23012 airfoil section; $\delta_f = 60°$; reference 41.

(b) NACA 23021 airfoil section; $\delta_f = 60°$; reference 42.

(c) NACA 64_1-212 airfoil section; reference 43.

FIGURE 43.—Contours of flap and vane positions for maximum section lift coefficient for several airfoil sections equipped with double slotted flaps.

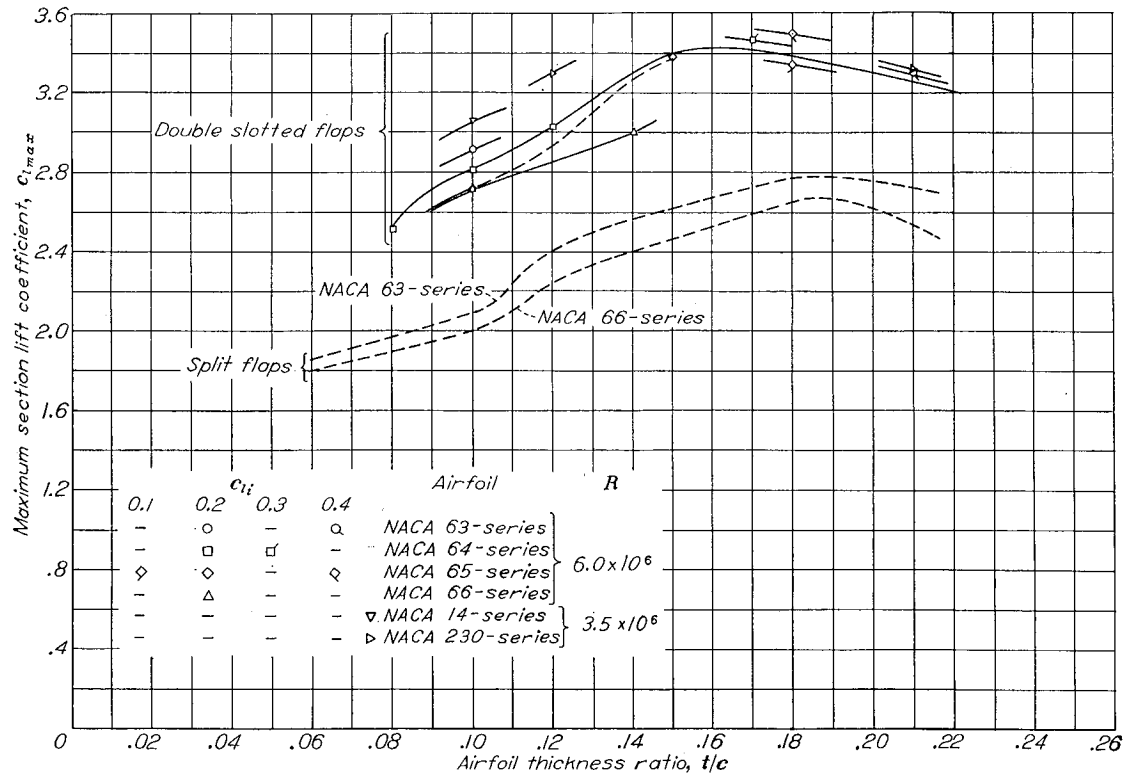

FIGURE 44.—Maximum section lift coefficients for several NACA airfoil sections with double slotted and split flaps.

Drag.—The drag characteristics of airfoils with double slotted flaps are perhaps best shown by a comparison with the drag of airfoils with single slotted flaps. Envelope polars for two single slotted flaps and a double slotted flap on the NACA 23012 airfoil are shown in figure 45. The drag coefficients at intermediate lift coefficients are considerably higher for the double slotted flap than for the single slotted flap. At higher lift coefficients, the drag of the airfoil with the double slotted flap is lower than that with the single slotted flap, principally because the separation of the air flow is delayed to higher lift coefficients. A similar comparison for various types of slotted flaps on the NACA 23021 airfoil is shown in reference 42. A comparison of envelope polars for the NACA 23012 and 23021 airfoils is shown in figure 46. The drag coefficients of the NACA 23012 section are lower than those of the NACA 23021 section for all lift coefficients below about 3.0; above this lift coefficient, there is very little difference between the two airfoils.

In the flap-retracted condition, double slotted flaps are subject to the same increments in minimum drag coefficient with flap retracted as single slotted flaps. In order to obtain lowest drag with flap retracted, every attempt should therefore be made to fair over the slot entry and to seal the flap gap in the retracted condition.

Pitching moment.—The pitching moments of airfoils with double slotted flaps should be similar to those of airfoils with single slotted flaps and should show the same sort of agreement with the thin-airfoil theory. There are not enough data available to show this effect completely since most of the double-slotted-flap data have been obtained with flaps of about the same size. Comparisons made with a few of the combinations for which data are available, however, show that the values of $\Delta c_m/\Delta c_l$ for double slotted flaps agree very well with those of single slotted flaps of the same size when the coefficients are defined on the basis of total chord.

Flap loads and moments.—Data on the aerodynamic loads over double slotted flaps on several airfoil sections are shown in references 45 and 50. The flap part of a double slotted flap is usually located geometrically in about the same position relative to the vane trailing edge as single slotted flaps are relative to the wing slot lip. The aerodynamic loads on these flaps are therefore of about the same order of magnitude as those on single slotted flaps. Vanes of double slotted flaps are effectively the leading-edge portions of highly deflected flaps and are usually highly cambered. For these reasons, the aerodynamic loads on these vanes are usually very high and normal-force coefficients as high as 5.0 have been measured on the vanes of highly deflected double slotted flaps.

Vanes of double slotted flaps are frequently located at positions where a large portion of their length extends under the wing slot lip. In such a position, with a converging passage all the way to the trailing edge of the slot lip, the minimum pressure is measured far back on the vane. Other double slotted flaps are so positioned that the vane is actually behind the wing slot lip and the pressure distribution reaches a peak at the vane leading edge. It may easily be seen from these considerations that the aerodynamic moment and the pressure chord forces on these vanes depend to a great extent on vane position and may vary over a very wide range. Flap and vane load characteristics for the airfoil double-slotted-flap combination, for which lift data are shown in figure 41, are presented in figure 47. These data show that flap and vane load characteristics for this configuration vary in a regular manner with flap deflection up to a deflection of 40°, at which deflection the lifts and flap loads cease to increase with deflection and the variation of flap loads with lift coefficient becomes erratic.

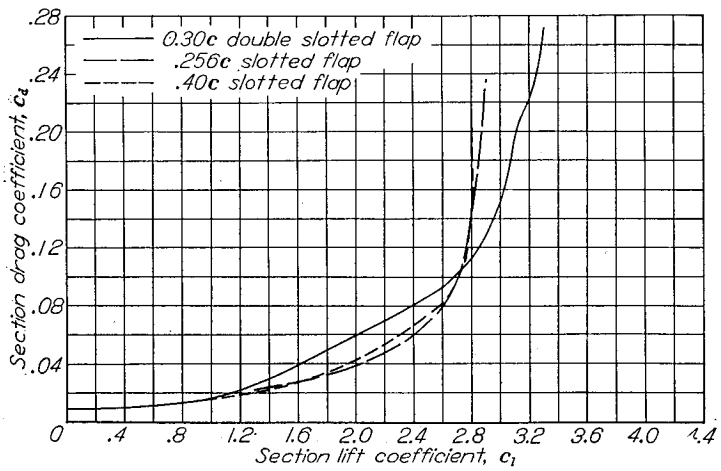

FIGURE 45.—Comparison of envelope polars for an NACA 23012 airfoil equipped with a double slotted flap and two sizes of single slotted flaps. R=3.5×10⁶; reference 41.

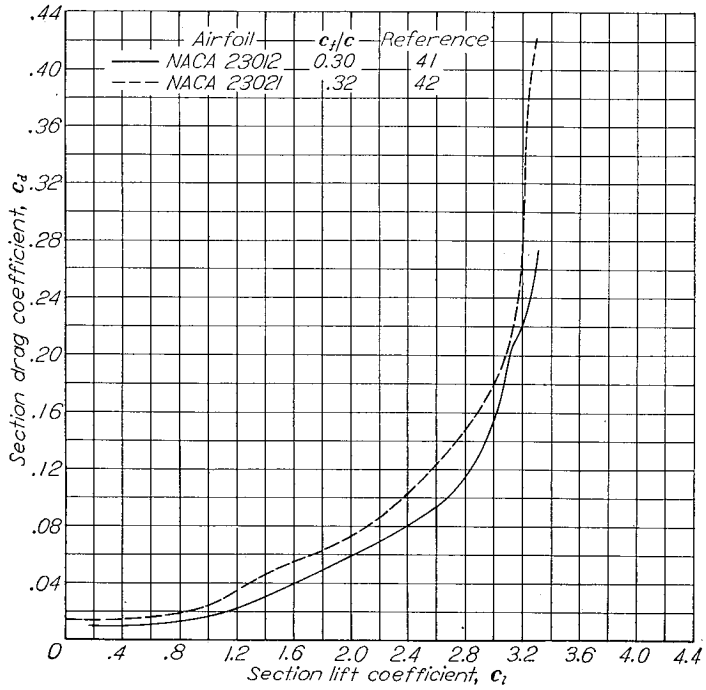

FIGURE 46.—Comparison of envelope polars for two airfoil sections equipped with double slotted flaps. R=3.5×10⁶.

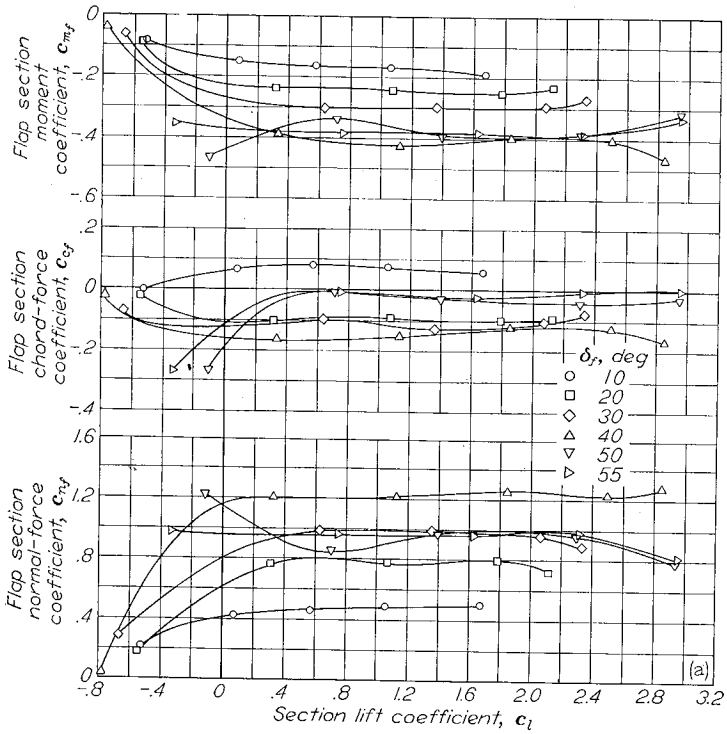

(a) Flap.

FIGURE 47.—Section force and moment characteristics for the double-slotted-flap arrangement on an NACA 63,4-421 (approx.) airfoil; partial slot-entry-skirt extension (see fig. 42 (b)). $R=2.4\times10^6$.

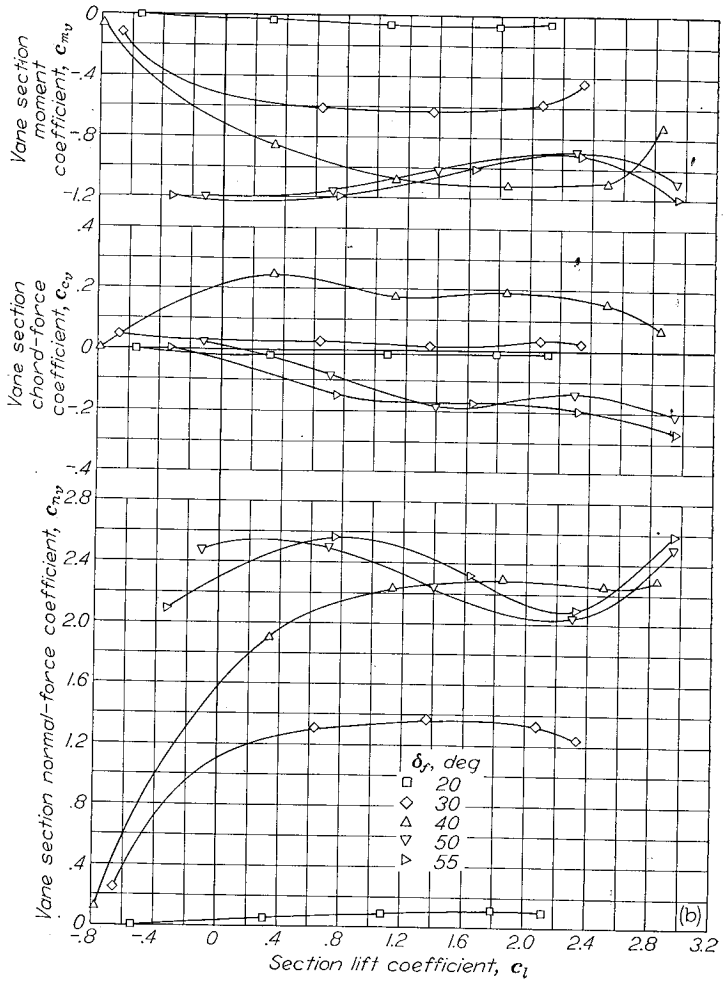

(b) Vane.

FIGURE 47.—Concluded.

EXTERNAL-AIRFOIL FLAPS AND VENETIAN-BLIND FLAPS

Two other devices, external-airfoil flaps and venetian-blind flaps, which operate on principles similar to slotted flaps are deserving of note although they are perhaps not as widely used as other types. External-airfoil flaps are actually separate lifting surfaces mounted externally to the wing near the trailing edge. For normal flight conditions the flap is kept at a small angle relative to the wing and for landing or take off the flap is deflected to a position very similar to that for an extensible slotted flap. Data are presented in references 12 and 52 to 56 for several airfoil sections equipped with external-airfoil flaps. Maximum lift coefficients of airfoils with external-airfoil flaps are shown to be similar to those obtained with slotted flaps of similar size when the coefficients are based on the area of the airfoil alone. Since the external-airfoil flap remains exposed to the air stream whereas the slotted flap is retracted to form the original airfoil contour, external-airfoil flaps produce slightly higher drag in the high-speed configuration than slotted flaps which provide the same maximum lift coefficient. Considerations of the flow around the airfoil and flap indicate that the external-airfoil flap should also be susceptible to icing hazards in the high-speed configuration. For these reasons (that is, no greater maximum lift than slotted flaps, high drag in the high-speed configuration, and possible icing problems) external-airfoil flaps have not been widely accepted although they offer some advantage over other types of flap in providing lateral control with a full-span flap.

Venetian-blind flaps are made up of a system of relatively small chord slats. Data are presented in references 57 and 58 for an NACA 23012 airfoil equipped with various venetian-blind-flap configurations. Variations in size and number of slats, deflection of the flap system as a whole, and individual deflections of the various slats were considered in these investigations. The data show that the multiple-slat flaps did not give significantly higher maximum lifts than a single slotted flap of the same total chord but gave considerably higher pitching moments.

SUMMARY OF SLOTTED-FLAP DATA

Slotted flaps are shown to provide higher maximum lift coefficients than any of the other devices discussed. Double slotted flaps are more efficient, particularly for airfoils of small thickness ratios, than single slotted flaps. Increases in total chord are shown to provide increases in maximum lift coefficients of single slotted flaps, whether obtained by increasing the flap size or increasing the slot-lip extension. Sharp corners or skirt extensions at the slot entry are shown to reduce the maximum lift coefficients of thick airfoils with slotted flaps although the entry condition seems to have

little effect on the maximum lift coefficients of thin airfoils with slotted flaps. Bending down the slot lip to direct the air flow down over the flap has been shown to have an advantageous effect on maximum lift coefficient. Data that are available seem to indicate that flap noses should have shapes similar to those of good airfoil sections. The best positions for highest maximum lift coefficients of double slotted flaps seem to fall within fairly well-defined limits although a few cases are shown where the best position falls outside these limits. The best positions of single slotted flaps are not so well defined. Maximum lift coefficients of both single and double slotted flaps are very sensitive to flap position, however, and optimum configurations cannot be predicted with any degree of accuracy.

Drags of airfoils with both single and double slotted flaps are lower than those of airfoils with plain or split flaps because the separation of the flow over the flap at relatively low deflections is prevented by the boundary-layer-control action of the slots. At a given lift coefficient, the drag of airfoils with slotted flaps is lowered if either the flap size or the slot-lip extension is increased. At moderate lift coefficients, the drag coefficients of double slotted flaps are higher than those of single slotted flaps.

Pitching moments of airfoils with both single and double slotted flaps are of the same order of magnitude as those shown by thin-airfoil theory if the pitching moments of the slotted flaps are defined on the basis of total chord with flap extended.

Normal-force coefficients of single slotted flaps or the flap parts of double slotted flaps are of approximately the same order of magnitude and usually reach maximum values of 1.6 or 1.8 at high flap deflections. Very high normal-force coefficients (as large as 5.0) are encountered on vanes of double slotted flaps, and aerodynamic moments and pressure chord forces can vary over wide ranges depending on vane position.

LANGLEY AERONAUTICAL LABORATORY,
NATIONAL ADVISORY COMMITTEE FOR AERONAUTICS,
LANGLEY FIELD, VA., *May 13, 1948.*

REFERENCES

1. Gustafson, F. B., and O'Sullivan, William J., Jr.: The Effect of High Wing Loading on Landing Technique and Distance, with Experimental Data for the B–26 Airplane. NACA ARR L4K07, 1945.
2. Glauert, H.: A Theory of Thin Aerofoils. R. & M. No. 910, British A.R.C., 1924.
3. Glauert, H.: Theoretical Relationships for an Aerofoil with Hinged Flap. R. & M. No. 1095, British A.R.C., 1927.
4. Pinkerton, Robert M.: Analytical Determination of the Load on a Trailing Edge Flap. NACA TN 353, 1930.
5. Theodorsen, T., and Garrick, I. E.: General Potential Theory of Arbitrary Wing Sections. NACA Rep. 452, 1933.
6. Allen, H. Julian: Calculation of the Chordwise Load Distribution over Airfoil Sections with Plain, Split, or Serially Hinged Trailing-Edge Flaps. NACA Rep. 634, 1938.
7. Abbott, Ira H., Von Doenhoff, Albert E., and Stivers, Louis S., Jr.: Summary of Airfoil Data. NACA Rep. 824, 1945.
8. Jacobs, Eastman N.: Tapered Wings, Tip Stalling, and Preliminary Results from Tests of the Stall-Control Flap. NACA ACR, Nov. 1937.
9. Ames, Milton B., Jr.: Wind-Tunnel Investigation of Two Airfoils with 25-Percent-Chord Gwinn and Plain Flaps. NACA TN 763, 1940.
10. Wenzinger, Carl J.: Wind-Tunnel Investigation of Ordinary and Split Flaps on Airfoils of Different Profile. NACA Rep. 554, 1936.
11. Wenzinger, Carl J., and Gauvain, William E.: Wind-Tunnel Investigation of an N.A.C.A. 23012 Airfoil with a Slotted Flap and Three Types of Auxiliary Flap. NACA Rep. 679, 1939.
12. Wenzinger, Carl J., and Harris, Thomas A.: Wind-Tunnel Investigation of an N.A.C.A. 23012 Airfoil with Various Arrangements of Slotted Flaps. NACA Rep. 664, 1939.
13. Abbott, Ira H., and Greenberg, Harry: Tests in the Variable-Density Wind Tunnel of the N.A.C.A. 23012 Airfoil with Plain and Split Flaps. NACA Rep. 661, 1939.
14. Wenzinger, Carl J., and Delano, James B.: Pressure Distribution over an N.A.C.A. 23012 Airfoil with a Slotted and a Plain Flap. NACA Rep. 633, 1938.
15. Wenzinger, Carl J., and Harris, Thomas A.: Wind-Tunnel Investigation of N.A.C.A. 23012, 23021, and 23030 Airfoils with Various Sizes of Split Flap. NACA Rep. 668, 1939.
16. Fullmer, Felicien F., Jr.: Wind-Tunnel Investigation of NACA 66(215)–216, 66,1–212, and 65_1–212 Airfoils with 0.20-Airfoil-Chord Split Flaps. NACA CB L4G10, 1944.
17. Harris, Thomas A., and Lowry, John G.: Pressure Distribution over an NACA 23021 Airfoil with a Slotted and a Split Flap. NACA Rep. 718, 1941.
18. Weick, Fred E., and Harris, Thomas A.: The Aerodynamic Characteristics of a Model Wing Having a Split Flap Deflected Downward and Moved to the Rear. NACA TN 422, 1932.
19. Platt, Robert C.: Aerodynamic Characteristics of a Wing with Fowler Flaps Including Flap Loads, Downwash, and Calculated Effect on Take-Off. NACA Rep. 534, 1935.
20. Harris, Thomas A., and Purser, Paul E.: Wind-Tunnel Investigation of an NACA 23012 Airfoil with Two Sizes of Balanced Split Flap. NACA ACR, Nov. 1940.
21. Lowry, John G.: Wind-Tunnel Investigation of an NACA 23012 Airfoil with Several Arrangements of Slotted Flaps with Extended Lips. NACA TN 808, 1941.
22. Harris, Thomas A.: Wind-Tunnel Investigation of an N.A.C.A. 23012 Airfoil with Two Arrangements of a Wide-Chord Slotted Flap. NACA TN 715, 1939.
23. Harris, Thomas A., and Swanson, Robert S.: Wind-Tunnel Tests of an NACA 23021 Airfoil Equipped with a Slotted Extensible and a Plain Extensible Flap. NACA TN 782, 1940.
24. Swanson, Robert S., and Schuldenfrei, Marvin J.: Wind-Tunnel Investigation of an NACA 23021 Airfoil with Two Sizes of Balanced Split Flaps. NACA ACR, Feb. 1941.
25. Wenzinger, Carl J., and Harris, Thomas A.: Wind-Tunnel Investigation of an N.A.C.A. 23021 Airfoil with Various Arrangements of Slotted Flaps. NACA Rep. 677, 1939.
26. Duschik, Frank: Wind-Tunnel Investigation of an N.A.C.A. 23021 Airfoil with Two Arrangements of a 40-Percent-Chord Slotted Flap. NACA TN 728, 1939.
27. Recant, I. G.: Wind-Tunnel Investigation of an N.A.C.A. 23030 Airfoil with Various Arrangements of Slotted Flaps. NACA TN 755, 1940.
28. Bogdonoff, Seymour M.: Tests of Two Models Representing Intermediate Inboard and Outboard Wing Sections of the XB–36 Airplane. NACA MR, Jan. 7, 1943.
29. Cahill, Jones F.: Two-Dimensional Wind-Tunnel Investigation of Four Types of High-Lift Flap on an NACA 65–210 Airfoil Section. NACA TN 1191, 1947.

30. Racisz, Stanley F.: Investigation of NACA $65_{(112)}$A111 (Approx.) Airfoil with 0.35-Chord Slotted Flap at Reynolds Numbers up to 25 Million. NACA TN 1463, 1947.

31. Loftin, Laurence K., Jr., and Rice, Fred J., Jr.: Two-Dimensional Wind-Tunnel Investigation of Two NACA Low-Drag Airfoil Sections Equipped with Slotted Flaps and a Plain NACA Low-Drag Airfoil Section for XF6U–1 Airplane. NACA MR L5L11, 1946.

32. Abbott, Ira H.: Tests of Four Models Representing Intermediate Sections of the XB–33 Airplane Including Sections with Slotted Flap and Ailerons. NACA MR, June 4, 1942.

33. Cahill, Jones F.: Aerodynamic Tests of an NACA 66(215)–116, $a=0.6$ Airfoil with a 0.25c Slotted Flap for the Fleetwings XA–39 Airplane. NACA MR L4K21, 1944.

34. Underwood, William J., and Abbott, Frank T., Jr.: Test of NACA 66,2–116, $a=0.6$ Airfoil Section Fitted with Pressure Balanced and Slotted Flaps for the Wing of the XP–63 Airplane. NACA MR, May 23, 1942.

35. Holtzclaw, Ralph W., and Weisman, Yale: Wind-Tunnel Investigation of the Effects of Slot Shape and Flap Location on the Characteristics of a Low-Drag Airfoil Equipped with a 0.25-Chord Slotted Flap. NACA MR A4L28, 1944.

36. Abbott, I. H.: Lift and Drag Characteristics of a Low-Drag Airfoil with Slotted Flap Submitted by Curtiss-Wright Corporation. NACA MR, Dec. 2, 1941.

37. Abbott, Ira H., and Turner, Harold R., Jr.: Lift and Drag Tests of Three Airfoil Models with Fowler Flaps Submitted by Consolidated Aircraft Corporation. NACA MR, Dec. 29, 1941.

38. Wenzinger, Carl J., and Anderson, Walter B.: Pressure Distribution over Airfoils with Fowler Flaps. NACA Rep. 620, 1938.

39. Harris, Thomas A., and Lowry, John G.: Pressure Distribution over an NACA 23021 Airfoil with a Slotted and a Split Flap. NACA Rep. 718, 1941.

40. Harris, Thomas A., and Recant, Isidore G.: Wind-Tunnel Investigation of NACA 23012, 23021, and 23030 Airfoils Equipped with 40-Percent-Chord Double Slotted Flaps. NACA Rep. 723, 1941.

41. Purser, Paul E., Fischel, Jack, and Riebe, John M.: Wind-Tunnel Investigation of an NACA 23012 Airfoil with a 0.30-Airfoil-Chord Double Slotted Flap. NACA ARR 3L10, 1943.

42. Fischel, Jack, and Riebe, John M.: Wind-Tunnel Investigation of an NACA 23021 Airfoil with a 0.32-Airfoil-Chord Double Slotted Flap. NACA ARR L4J05, 1944.

43. Cahill, Jones F., and Racisz, Stanley F.: Wind-Tunnel Investigation of Seven Thin NACA Airfoil Sections to Determine Optimum Double-Slotted-Flap Configurations. NACA TN 1545, 1948.

44. Quinn, John H., Jr.: Tests of the NACA 64_1A212 Airfoil Section with a Slat, a Double Slotted Flap, and Boundary-Layer Control by Suction. NACA TN 1293, 1947.

45. Visconti, Fioravante: Wind-Tunnel Investigation of Air Loads over a Double Slotted Flap on the NACA 65(216)–215, $a=0.8$ Airfoil Section. NACA RM L7A30, 1947.

46. Bogdonoff, Seymour M.: Wind-Tunnel Investigation of a Low-Drag Airfoil Section with a Double Slotted Flap. NACA ACR 3I20, 1943.

47. Quinn, John H., Jr.: Wind-Tunnel Investigation of Boundary-Layer Control by Suction on the NACA 65_3–418, $a=1.0$ Airfoil Section with a 0.29-Airfoil-Chord Double Slotted Flap. NACA TN 1071, 1946.

48. Quinn, John H., Jr.: Wind-Tunnel Investigation of the NACA 65_4–421 Airfoil Section with a Double Slotted Flap and Boundary-Layer Control by Suction. NACA TN 1395, 1947.

49. Braslow, Albert L., and Loftin, Laurence K., Jr.: Two-Dimensional Wind-Tunnel Investigation of an Approximately 14-Percent Thick NACA 66-Series-Type Airfoil Section with a Double Slotted Flap. NACA TN 1110, 1946.

50. Cahill, Jones F.: Aerodynamic Data for a Wing Section of the Republic XF–12 Airplane Equipped with a Double Slotted Flap. NACA MR L6A08a, 1946.

51. Nuber, Robert J., and Rice, Fred J., Jr.: Lift Tests of a 0.1536c Thick Douglas Airfoil Section of NACA 7-Series Type Equipped with a Lateral-Control Device for Use with a Full-Span Double-Slotted Flap on the C–74 Airplane. NACA MR L5C24a, 1945.

52. Platt, Robert C.: Aerodynamic Characteristics of Wings with Cambered External-Airfoil Flaps, Including Lateral Control with a Full-Span Flap. NACA Rep. 541, 1935.

53. Platt, Robert C., and Abbott, Ira H.: Aerodynamic Characteristics of N.A.C.A. 23012 and 23021 Airfoils with 20-Percent-Chord External-Airfoil Flaps of N.A.C.A. 23012 Section. NACA Rep. 573, 1936.

54. Wenzinger, Carl J.: Pressure Distribution over an N.A.C.A. 23012 Airfoil with an N.A.C.A. 23012 External-Airfoil Flap. NACA Rep. 614, 1938.

55. Noyes, Richard W.: Wind-Tunnel Tests of a Wing with a Trailing-Edge Auxiliary Airfoil Used as a Flap. NACA TN 524, 1935.

56. Platt, Robert C., and Shortal, Joseph A.: Wind-Tunnel Investigation of Wings with Ordinary Ailerons and Full-Span External Airfoil Flaps. NACA Rep. 603, 1937.

57. Wenzinger, Carl J., and Harris, Thomas A.: Preliminary Wind-Tunnel Investigation of an N.A.C.A. 23012 Airfoil with Various Arrangements of Venetian-Blind Flaps. NACA Rep. 689, 1940.

58. Rogallo, F. M., and Spano, Bartholomew S.; Wind-Tunnel Investigation of an N.A.C.A. 23012 Airfoil with 30-Percent-Chord Venetian-Blind Flaps. NACA Rep. 742, 1942.

○

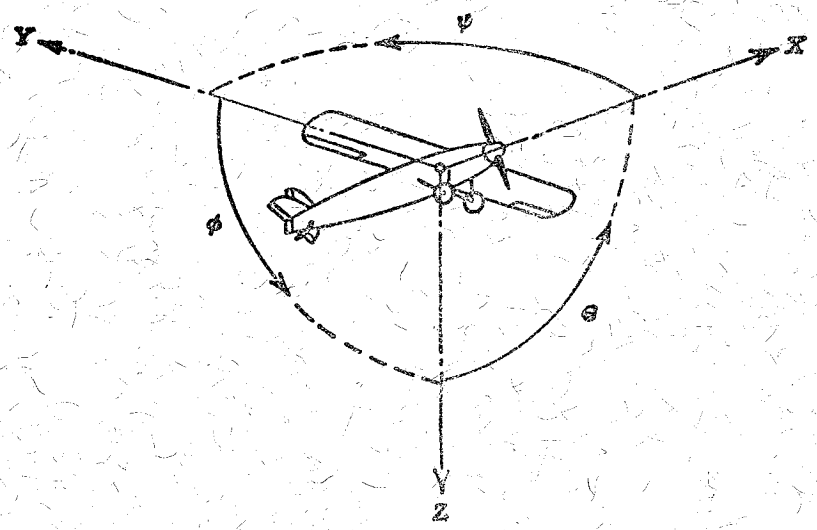

Positive directions of axes and angles (forces and moments) are shown by arrows

Axis		Force (parallel to axis) symbol	Moment about axis			Angle		Velocities	
Designation	Symbol		Designation	Symbol	Positive direction	Designation	Symbol	Linear (component along axis)	Angular
Longitudinal	X	X	Rolling	L	$Y \longrightarrow Z$	Roll	ϕ	u	p
Lateral	Y	Y	Pitching	M	$Z \longrightarrow X$	Pitch	θ	v	q
Normal	Z	Z	Yawing	N	$X \longrightarrow Y$	Yaw	ψ	w	r

Absolute coefficients of moment

$C_l = \frac{L}{qbS}$ (rolling) $\quad C_m = \frac{M}{qcS}$ (pitching) $\quad C_n = \frac{N}{qbS}$ (yawing)

Angle of set of control surface (relative to neutral position), δ. (Indicate surface by proper subscript.)

4. PROPELLER SYMBOLS

D Diameter

p Geometric pitch

p/D Pitch ratio

V' Inflow velocity

V_s Slipstream velocity

T Thrust, absolute coefficient $C_T = \frac{T}{\rho n^2 D^4}$

Q Torque, absolute coefficient $C_Q = \frac{Q}{\rho n^2 D^5}$

P Power, absolute coefficient $C_P = \frac{P}{\rho n^3 D^5}$

C_s Speed-power coefficient $= \sqrt[5]{\frac{\rho V^5}{P n^2}}$

η Efficiency

n Revolutions per second, rps

Φ Effective helix angle $= \tan^{-1}\left(\frac{V}{2\pi r n}\right)$

5. NUMERICAL RELATIONS

1 hp=76.04 kg-m/s=550 ft-lb/sec

1 metric horsepower=0.9863 hp

1 mph=0.4470 mps

1 mps=2.2369 mph

1 lb=0.4536 kg

1 kg=2.2046 lb

1 mi=1,609.35 m=5,280 ft

1 m=3.2808 ft